Influence of light and algae on nutrient transformations at the sediment-water interface of an agricultural stream

Jenae Elizabeth Pinney

Thesis submitted to the faculty of the

Virginia Polytechnic Institute and State University

in partial fulfillment of the requirements for the degree of

Master of Science

In

Biological Systems Engineering

Durelle Scott, Chair

Cully Hession

Daniel Gallagher

May 27, 2011

Blacksburg, VA

Keywords: Nutrient Retention, Nitrate, Phosphorus, Ammonium, DOM

Influence of light and algae on nutrient transformations at the sediment water interface of an agricultural stream

Jenae Elizabeth Pinney

Abstract

The sediment-water interface is an active biogeochemical zone within streams, where solutes come in contact with mineral surfaces, biota, and reducing conditions. Here, we sought to examine the influence of light, the sediment water interface, and algae on dissolved organic carbon (DOC), nitrogen, and phosphorus within Maple Creek, an agriculturally impacted stream located in Fremont, Nebraska. Simultaneous continuous injection experiments into replicate open- and closed-bottom chambers were used to control the hydrologic residence time. A bromide tracer was injected, and samples were taken for nutrient analysis in the surface and subsurface water at depths up to 8 cm. Dissolved oxygen (DO) and temperature were recorded in order to monitor biotic production. Experiments were conducted over 10 hours, encompassing both light and dark conditions. Results show a strong biotic influence at the sediment-water interface causing nutrient uptake and changes in carbon quality. Changes are especially pronounced during peak photosynthesis hours. The open-bottom mesocosms consistently showed removal of N and P from the surface water to the subsurface. An increase in DOC flux was observed in the open-bottom mesocosms and the organic matter pool exhibited evidence of microbial reduction. The closed-bottom mesocosm showed NH_4^+ increased likely due to photochemical oxidation. These results show the importance of promoting exchange through the subsurface and across the sediment-water interface due to the positive impact it has on nutrient retention.

Acknowledgements

I would like to thank my committee for their guidance and insightfulness throughout this project. I would also like to thank Dr. Charles Sharpless and Dr. Ben Kisila for giving me the opportunity to start my research adventures with them and paving my future with new opportunities. I would like to thank all the graduate and undergraduate students, faculty and staff I got to work with throughout my time at Virginia Tech. They all made work enjoyable and were always willing to help whenever it was needed. I would also like to thank my family and friends for all their support throughout the years. I cherish the great memories you have given me and I could not complete my goals without you.

Table of Contents

List of Figures

List of Tables

Chapter 1 - Introduction

Background and Motivation

The number of streams, estuaries, and lake ecosystems affected by eutrophication-derived hypoxia has increased worldwide. Surface waters experiencing excess nutrient levels can suffer from eutrophication and, in turn, dangerously low dissolved oxygen (DO) levels. Eutrophication-derived hypoxic events of coastal and estuarine systems have been shown to cause mass mortality (dead zones) and major changes in community structure (e.g. changes in productivity, fishkills, etc.) [*Diaz and Rosenberg*, 1995; 2008]. Human health becomes a concern as nitrate (NO_3^-) levels above 10 mg/L as N can cause methemoglobinemia (or "blue baby syndrome"). Blooms of cyanobacteria release toxins causing illness and even death in humans and animals [*Carmichael*, 2001; *Hawkins et al.*, 1985]. In the U.S., the annual cost of eutrophication has been estimated as approximately $2.2 billion dollars due to loss of property value, loss of recreational activities, drinking water cleaning costs, and recovery costs for endangered or threatened species [*Dodds et al.*, 2009].

The number of dead zones worldwide has essentially doubled each decade since the 1960s with over 400 estuaries currently documented as impacted by hypoxia [*Diaz and Rosenberg*, 2008]. Declining DO concentrations have lagged ten years behind the use of industrially produced fertilizer [*Diaz and Rosenberg*, 2008; *Galloway et al.*, 2008].Throughout the U.S., groundwater wells monitored by the USGS have seen nutrient increases since the early 1990's and groundwater recharge estimates show nitrogen began increasing around 1975 when fertilizer application was first used in the U.S. [*Dubrovsky and Hamilton*, 2010]. The USGS National Water-Quality Assessment program (NAWQA) showed this upward trend is not due to variations in precipitation or streamflow but is directly related to anthropogenic influences on the

landscape (e.g. atmospheric deposition, fertilizer and manure applications) [*Dubrovsky and Hamilton,* 2010].

Only 4% of the worldwide hypoxic systems exhibited signs of improvement at the end of the 20th century [*Diaz and Rosenberg,* 2008]. Despite this low number, there is evidence improvement and recovery are possible with reductions in organic matter and nutrient loadings as seen with the remediation of the Black Sea [*Mee,* 2006]. Demersal fish within the black sea were greatly diminished from eutrophication-derived hypoxia until 1989 when the collapse of communist regions in Eastern Europe caused a decrease in economic capital [*Mee,* 2006]. Farmers suddenly did not have money for fertilizers and animal farms closed [*Mee,* 2006]. This drastic decrease in nutrient inputs allowed the ecosystem to recover and hypoxia disappeared in the 1990s [*Diaz and Rosenberg,* 2008; *Mee,* 2006]. In the U.S., the Gulf of Mexico has experienced localized hypoxia since the 1970s with the spatial extent increasing over the years [*Diaz and Rosenberg,* 2008; *Rabalais et al.,* 2001]. From 1985 to 1992, the average size of hypoxia was 8,200 km^2 [*Rabalais et al.,* 2007a]. This increased to an average of 15,900 km^2 from 1992 to 2007 [*Rabalais et al.,* 2007a] but when freshwater discharge from the Mississippi River is low, the Gulf of Mexico experiences decreased spatial extent of hypoxia due to decreased nutrient loadings from the "breadbasket" [*Diaz and Rosenberg,* 2008; *Rabalais et al.,* 2007b]. These examples provide hope for remediation efforts even with the incredible spatial extent of hypoxia plaguing the Gulf of Mexico.

Remediation efforts for hypoxic areas require land management practices to reduce nutrient export from watersheds. Once nutrients reach surface waters, cleanup becomes difficult because hydraulic residence times are very short making physical, chemical, and biological retention harder to achieve. Remediation of surface waters also requires nutrient removal within the stream

network. When implemented properly, management practices help protect human health and prevent ecosystem damage from eutrophication-derived hypoxia but not every attempt has been successful. There is a lack of complete mechanistic understanding about the biogeochemistry controlling the fate and transport of nutrients within stream systems, part of which is due to the lack of DOM characterization completed within studies [*Jaffe et al.*, 2008]. Having a better understanding of the processes responsible for altering, transferring, and storing nutrients within a stream system will further the understanding of nutrient retention and transport downstream. Eutrophication and hypoxic conditions could then be controlled downstream as this knowledge is used to develop more effective management practices.

NO_3^- and phosphorus (P) have received the most attention for management because they are commonly the limiting nutrient for freshwater systems. Most agricultural and urban streams throughout the nation have NO_3^- and P concentrations between two and ten times greater than USEPA recommended criteria [*Dubrovsky and Hamilton*, 2010]. NO_3^- management is perhaps the biggest concern since 5-50% (depending mostly on geology, soil hydrology, and agricultural practices) of NO_3^- input from nonpoint pollution sources (NPS) are exported out of watersheds [*Dubrovsky and Hamilton*, 2010]. The amount of NO_3^- exported has increased as terrestrial ecosystems become increasingly nitrogen-saturated [*Mulholland et al.*, 2008]. Nitrogen can be removed from the system by biotic (e.g. assimilation, denitrification) or abiotic (e.g. dissimilatory nitrate reduction to ammonium (DNRA), nitrate reduction coupled to iron oxidation) pathways. Attempts have been made to quantify denitrification rates (e.g. [*Mulholland et al.*, 2006], [*Hedin et al.*, 1998]) since denitrification is the only pathway to remove NO_3^- from the system by turning it into gaseous N_2. In order for denitrification to occur, anoxic conditions need to exist. Nitrification (biological process oxidizing NH_4^+ to NO_3^-) and denitrification may

co-occur in the same area due to some pore spaces having anoxic conditions [*Sheibley et al.*, 2003]. Quantifying these processes is important because biota can immobilize not only NO_3^- but also ammonium (NH_4^+), phosphate (PO_4^{3-}), and carbon since biota require these to grow.

The nitrogen and P cycles directly influence each other due to their biotic link. P has a strong attraction to sediment so it is usually not exported as rapidly as NO_3^- which typically makes it the limiting nutrient for biological reactions. The P cycle is less complex than the nitrogen cycle because there are only two main pathways P can be removed from the stream system. P can either be assimilated into biota or sorbed to sediment. The nitrogen cycle could not occur without an electron donor. Typically carbon is used as the electron donor, for example when reducing NO_3^- to gaseous N_2 during denitrification. Carbon is also created by biota during respiration so the carbon and nitrogen cycles along with the P cycle are intimately linked. Understanding their interactions is therefore vital to estimating nutrient removal within streams.

Dissolved organic matter (DOM) is one of the largest sources of biologically available organic carbon [*Fellman et al.*, 2010; *Keil and Kirchman*, 1991; *Wetzel*, 1992] used in heterotrophic metabolism. DOM is made up of a complicated mixture of carbon from multiple sources. Recent advancements in spectroscopic techniques have opened a new door to studying the influence of biota on nutrients. DOM can now be easily classified using absorption and fluorescence information as well as parallel factor analysis (PARAFAC) [*Fellman et al.*, 2010; *McKnight et al.*, 2001]. The biochemical composition of DOM is what determines its reactivity and ability to be metabolized by organisms [*Fellman et al.*, 2010]. Fluorescence offers the ability to determine DOM source, redox state and biological reactivity [*Miller et al.*, 2009b; *Stedmon et al.*, 2003] which is incredibly useful in understanding the biogeochemical processes occurring

within a stream. Characterizing the DOM utilized and produced by autotrophs and heterotrophs will help quantify nutrient removal within a stream system.

The sediment-water interface of streams and the hyporheic zone have been identified as hot spots of particular interest for nutrient and carbon transformations. The microtopography of streams creates downwelling areas where surface-water enters the hyporheic zone (e.g. riffles) before later returning in an upwelling zone (e.g. pools). Total nutrient removal within a stream could be estimated by scaling up the nutrient removal occurring on these smaller riffle and pool scales. Numerous studies have looked at various parts of the hydrologic and biogeochemical processes in stream field experiments (e.g. [*Puckett et al.*, 2008], [*Triska et al.*, 1989], [*Thouin et al.*, 2009] and several others) and in the lab (e.g. [*Sheibley et al.*, 2003], [*Turlan et al.*, 2007], [*Mermillod-Blondin et al.*, 2005] and several others) to try to quantify nutrient removal. Hedin et al. [1998] estimated 30-60% NO_3^- retention at the sediment-water interface is due to denitrification and Mulholland et al. [2008] estimated 16% of total NO_3^- uptake was due to denitrification. Mulholland et al. [2008] also found photoautotrophs played an important role in NO_3^- removal because total uptake velocity increased with gross primary production. Baker et al. [1999] found the most DOC retention occurred via anaerobic pathways with denitrification. The importance of hydrologic factors has also been shown with a negative relationship between travel time and retention [*Alexander et al.*, 2000; *Baker et al.*, 1999]. Being able to predict and quantify nutrient and DOM processes across the sediment-water interface would further the understanding of what management practices need to be in place. This information will also help determine what impact climate change could have on nutrient fate and transport.

Climate change models are predicting freshwater discharges will increase agricultural nutrient loads to coastal ecosystems [*Diaz and Rosenberg*, 2008]. Current estimates show a 20%

increase in discharge for the Mississippi River would occur, leading to a 20-60% decrease in subpycnocline DO and expanding the oxygen depleted area [*Diaz and Rosenberg*, 2008]. Currently, spring snowmelt results in an acute stream acidification event. In the Catskill and Adirondack Mountains, the annual average pH of rain and snow is 4.3 [*Murdoch and Stoddard*, 1992]. With glaciers receding and snow accumulations decreasing, there are worries stream ecosystems could be negatively impacted if acidification events decrease. There are, however, predictions of less frequent but more severe summer storm events increasing stream acidity due to the 'wash out' of more nitrate and sulfate deposits [*Moore et al.*, 1997]. Currently, the impact of acute stream acidification events on nutrient retention is not well understood. It is important to understand how nutrient removal within stream systems is impacted by the acidification process. If the nitrogen, P, and carbon cycles are significantly impacted, management practices will have to be developed to incorporate these changes.

Research Objectives

The goal of this study was to improve the fundamental knowledge of biogeochemical processes controlling nutrient fate and transport across the sediment-water interface into the subsurface of agriculturally impacted streams. This knowledge will be used to improve water quality and remediation designs. This goal was achieved by determining the amount of nutrient retention occurring across the sediment-water interface of a nitrogen enriched stream. The effect of light, autotrophs, and DOM on nutrient retention were also quantified. The specific objectives were:

1) Evaluate if the presence of biota significantly changes the ability of the hyporheic zone to retain nutrients (NO_3^-, NH_4^+, total dissolved nitrogen (TDN), PO_4^{2-} and DOM, primarily the dissolved organic carbon (DOC) and dissolved organic nitrogen (DON) fractions.)
2) Evaluate if DOM quality changes during peak sunlight hours.
3) Evaluate if a decrease in pH changes the ability of the hyporheic zone to retain nutrients.

To test these research objectives, the following hypotheses were developed:

1) The presence of biota causes a gain in DOC and an increase in nitrogen (N), and P retention due to uptake.
2) Sunlight causes an increase in N and P retention due to uptake from photosynthetic processes.
3) Sunlight causes a change in DOM quality from a more microbially derived DOM during the day to a more terrestrially derived DOM at night due to the autotrophic community.
4) A reduction in pH will have no effect on N retention, but P and DOC concentrations will increase due to the reduction of iron releasing sorbed particles.

Chapter 2 – Materials and Methods

Site Description

Maple Creek is a tributary to Elkhorn River located in eastern Nebraska. It has a watershed area of 956 km^2 [*Puckett et al.*, 2008] and was chosen due to the watershed's predominantly agricultural (corn and soybean) land use, representative of many Midwest watersheds [*Puckett et al.*, 2008]. Nitrogen use within the watershed was estimated to be 4666 Mg (51 kg/ha) in 2003 [*Fredrick et al.*, 2006; *Puckett et al.*, 2008] creating a heavily N-enriched stream environment based on national background values defined by Fuhrer et al [1999]. The riverbed is generally homogenous consisting of sand with some gravel (particle-size analysis revealed the majority of

the riverbed was between 0.15 and 0.50 mm) which results from the parent material of eolian sand, silt, and loess soil [*Puckett et al.*, 2008]. Experiments were conducted near Fremont, Nebraska directly upstream of a USGS gage (site 06800000) in July of 2009 (Figure 1). The field experiment was conducted during summer baseflow conditions where there was minimal discharge fluctuation. Discharge remained between 1.58 and 1.61 m^3/s for all field experiments (Figure 2**Error! Reference source not found.**). Climate within eastern Nebraska is typically humid with hot summers and cold winters [*Puckett et al.*, 2008]. For July 2009, NOAA's annual climatological summary for Fremont Nebraska shows the mean temperature was 21.8°C and the mean precipitation was 39.9 mm which was slightly below normal.

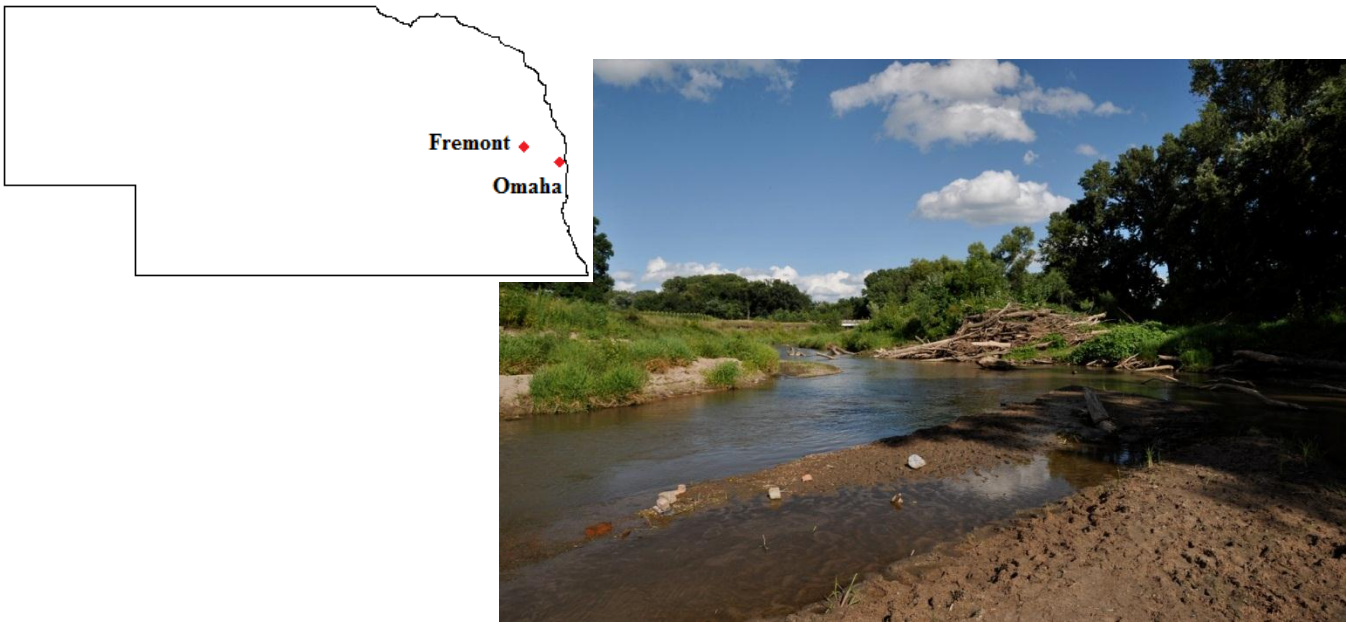

Figure 1: Location and photograph of Maple Creek located in Fremont, Nebraska. Picture taken by Durelle Scott.

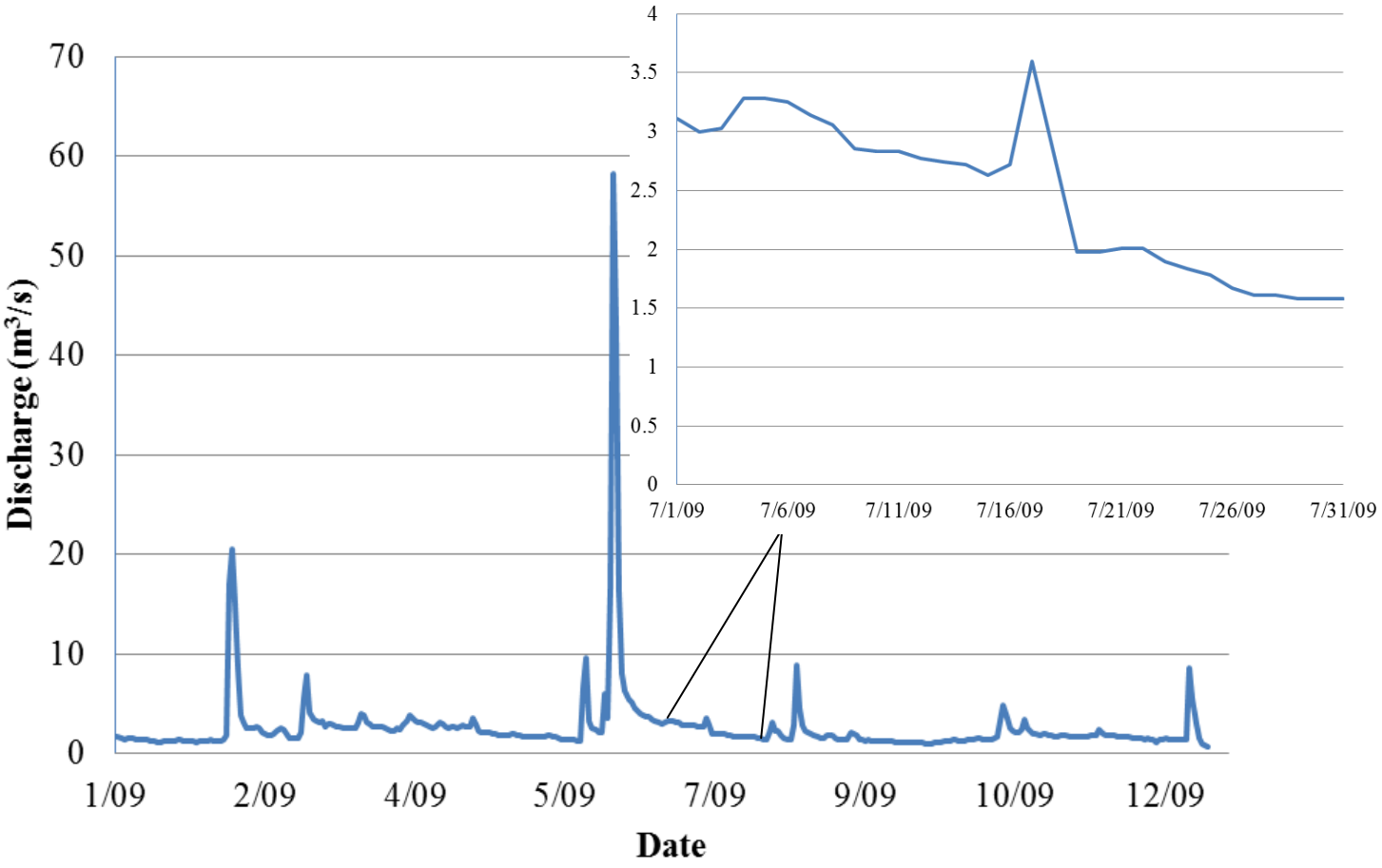

Figure 2: USGS daily mean discharge data for Maple Creek for the 2009 calendar year. Data is from USGS site 06800000 located near Nickerson, Nebraska.

Field Methods

With the riverbed being essentially homogenous, the hydrologic flow from the surface to the subsurface was controlled throughout each experiment using mesocosms. Two open-bottom mesocosms (46 cm inner diameter, 61 cm height)) made of Solacryl® SUVT (Spartech Company), UV-transparent plexiglas, were inserted into the streambed to a depth of approximately 20 cm (Figure 3). One closed-bottom mesocosm was placed within the stream alongside the open-bottom mesocosms. Streamwater was injected into each mesocosm with a flow rate of approximately 60 mL/min chosen to achieve a surface-water residence time of approximately 300 min. The flow rate provided a steady head slightly above the water level of

the surrounding stream (Figure 3). Another pump circulated the surface water to maintain a homogenous surface water mixture to prevent concentration gradients from forming in the surface-water while also minimizing sediment resuspension. The closed-bottom mesocosm also contained a pump to remove water at a slow and constant rate so the water residence time remained consistent with the open-bottom mesocosms throughout the experiment. To be sure diffusion-controlled effects were eliminated from the mesocosms, a rhodamine dye test was conducted within the closed-bottom mesocosm prior to setting up for field experiments to verify complete mixing of input water was obtained within 20 s of addition.

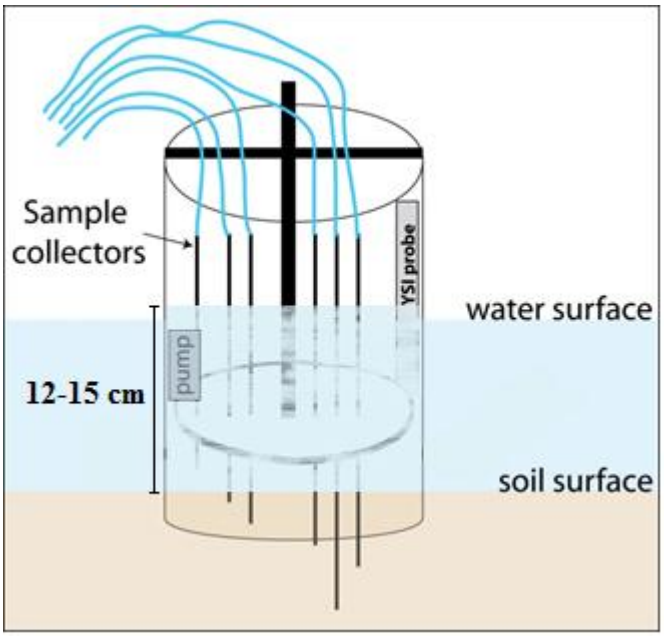

Figure 3: Set-up for the open-bottom mesocosms. Samples were collected at the sediment-water interface (depth of 0 cm), 1.5 cm, 3.0 cm, 5.0 cm, and 8.0 cm.

The injected streamwater was prefiltered (10µm) prior to the start of the experiment to remove any large algae and sediment that may clog sample lines. The water was stored in a reservoir under a reflective cover in the stream to maintain chemical and thermal composition. Streamwater injection from the reservoir was continuously pumped into the open-bottom

mesocosms throughout the night before experiments in order for each mesocosm to equilibrate. At the start of chemical sampling, a bromide slug was added to each mesocosm, and immediately followed with a constant bromide injection in order to quantify subsurface flowpath residence times.

Filtered water samples (0.20 μm) were taken from each mesocosm using a MINIPOINT sampler [*Duff et al.*, 1998] at the sediment-water interface and various depths (1.5 cm, 3.0 cm, 5.0 cm, and 8.0 cm) along the subsurface flowpaths. Samples were obtained at a pumping rate of 1.5 mL/min to maintain sample integrity [*Duff et al.*, 1998]. Samples were taken at least twice an hour with more rapid collection occurring within the first two hours to obtain bromide breakthrough curves. Upon collection, nutrient samples were stored on dry-ice and frozen until analysis.

The experiment, which was repeated 3 times over four days, lasted approximately ten hours each. Peak sunlight hours and nighttime conditions were captured by the experiment in order to contrast light and dark conditions. Differences between the closed-bottom and open-bottom mesocosms were used to determine the impact of the sediment-water interface, and which processes dominate within the water column versus the subsurface. Visual inspection of the mesocosms determined there was more biotic growth present at the start of the experiment on day 2. On day 3, the mesocosm walls and sediment were cleaned of as much biofilm as possible before the experiment to examine the impact caused by the absence of biota. The pH was adjusted in the closed-bottom mesocosm and one open-bottom mesocosm from the naturally basic stream water (pH of approximately 8.5) to acidic conditions (pH of approximately 6.5). The treatments for each mesocosm and their acronym are summarized in Table 1. DO, pH, temperature, and conductivity of the mesocosms were monitored with YSI multiprobes.

Continuous measurements were taken with a YSI in one of the open-bottom mesocosms while point measurements were taken every hour within the other open-bottom mesocosm and the closed-bottom mesocosm.

Table 1: Summary of mesocosm treatments and their acronym.

Mesocosm Type	Treatment	Acronym
Open-bottom	None	MO
Open-bottom	Biota removed	MO-c
Open-bottom	Acidified and biota removed	MO-ac
Closed-bottom	None	MC
Closed-bottom	Acidified and biota removed	MC-ac

Laboratory Analysis

Sample Preparation and Analysis

Stream samples were collected for analyses of Br^-, NO_3^-, PO_4^{3-}, NH_4^+, DOC, and TDN. A summary of the instrumentation, method, and detection limit for each water quality constituent is provided in (Table 2). Since NO_3^- analysis utilized the conversion of NO_3^- to NO_2^-, the reported NO_3^- concentrations actually refer to the NO_x sample content and will from now on be referenced as NO_x. DON was determined by subtracting the sum of the inorganic nitrogen (NO_x and NH_4^+) from TDN.

Table 2: Water quality analysis instrumentation, methods, and detection limits.

Constituent	Instrumentation	Method	APHA Method #	Detection Limit
Bromide (Br^-)	Dionex ICS-3000 (Sunnyvale, CA)	Ion chromotography	4110 B	0.10 mg/L
Ortho-Phosphorus (PO_4^{2-}-P)	SEAL Autoanalyzer 3 (Mequon, WI)	Murphy & Riley colorimetric method with ascorbic acid reduction	4500-P G	3.72 µg/L
Nitrate+Nitrite (NO_3-N)	SEAL Autoanalyzer 3 (Mequon, WI)	Copper-Cadmium reduction	4500-NO_3 I	0.034 mg/L †
Ammonium (NH_4^+)	SEAL Autoanalyzer 3 (Mequon, WI)	Salicylate colorimetric reaction	4500-NH_3 H	10.51 µg/L
Non-Purgeable Organic Carbon (DOC)	Shimadzu TOC Analyzer (Columbia, MD)	Acidification and Combustion	5310 D/B	46 µg/L †
Total Dissolved Nitrogen	Shimadzu TOC Analyzer (Columbia, MD)	Acidification and Combustion	5310 B	20 µg/L †

† Detection limit as stated by the instrument manual. All other detection limits were determined via instrument analysis.

Fluorescence Spectroscopy and PARAFAC Modeling

A fluorometer (Fluoromax-4 Spectrofluorometer; Horiba Jobin Yvon, Edison, NJ) was used to measure fluorescence. Samples were diluted with Milli-Q water in order to avoid inner filter effects [*Fellman et al.*, 2009; *Green and Blough*, 1994]. For constant excitation wavelength emission scans, an integration time of 0.25 s was used. EEMs were created in ratio mode by measuring excitation from 240-450 nm (every 5 nm) and emission from 350-550 nm (every 2 nm). A 1 cm cell width was used and excitation and emission slit widths were 5 nm. EEMs were corrected for instrument bias and Raman normalized using a MATLAB program (MATLAB 7.11.0, Mathworks). Suwanee River and Pony Lake samples were analyzed using the same procedure to verify the results since these samples have been well studied [*Brown et al.*, 2004;

McKnight et al., 2001]. Details of the fluorescence approach can be found elsewhere [*Cory et al.*, 2010]. The corrected EEMs were then analyzed using a parallel factor analysis (PARAFAC) model following the procedures of [*Cory and McKnight*, 2005]. PARAFAC analysis was conducted in Matlab using the "N-way toolbox for MATLAB version 2.10". (C. A. Andersson and R. Bro. The N-way Toolbox for MATLAB. Chemom.Intell.Lab.Syst. 52 (1):1-4, 2000.).

Data Analysis

A breakthrough curve was developed using the bromide time-series data. Since input flow rates and the water level were kept constant, residence times for each mesocosm were determined using the equation [*Dingman*, 2002]:

$$T_r = V_m/Q_{out}$$

where V_m is the water volume in the mesocosm (mL) and Q_{out} is the volumetric flow rate out of the mesocosm (mL/min), which is assumed to be the volumetric flow rate into the mesocosm. Mean travel times calculated from the bromide breakthrough curves were used to estimate residence time for each depth. Time-series data of the cumulative mass flux for nutrients (NO_x, PO_4^{3-}, NH_4^+, TDN, DOC) at the inlet (sediment-water interface) and outlet (depth of 8 cm) were fit to linear models to determine whether nutrients were gaining or losing along the subsurface flowpath. Any concentration below the minimum detection limit was, for calculation purposes, labeled as zero. Since the dataset is a cumulative load that starts at zero, a linear regression model forcing the intercepts through zero was used. The slope of this linear model was the quantification of the change in mass flux over time, or the retention (or gaining) rate.

PARAFAC model results were used to determine DOM characterization for MO-ac, MO, and MC-a from several depth profiles taken at various times throughout the day 3 experiment. DOM composition was determined from the PARAFAC determined percent of thirteen distinct

components present as defined in Cory and McKnight [2005] and Miller et al [2006]. Redox index (RI), fluorescence index (FI), and specific ultraviolet absorbance (SUVA) were also determined for these profiles. RI was determined from the PARAFAC model [*Miller et al.*, 2006] while FI and SUVA were determined as outlined in McKnight et al. [2001] and Weishaar et al. [2003], respectively.

Results were analyzed using a balanced three-way ANOVA to determine how SUVA, RI, FI, and protein composition changed as a function of depth, time, and mesocosm treatments (normal pH or acidified) between MO-ac and MO. Once a relationship was determined to be present from the ANOVA results, a Tukey HSD test was used to determine which differences were significant. A balanced two-way ANOVA was then used to determine how SUVA, RI, FI, and protein composition changed as a function of time and mesocosm treatments (normal or acidified stream pH) for the surface waters of MO-ac, MO, and MC-ac. SUVA analysis for the subsurface waters was initially unbalanced since one point (MO at time 14:30 at depth 1.5 cm) did not have enough sample to be analyzed. To maintain a balanced analysis, a SUVA value was calculated using the average of other 1.5 cm values for MO on that day. ANOVA analyses were completed using R (R Development Core Team, Vienna, Austria), and the Tukey HSD tests were generated using an ANCOVA within SAS software, Version 9.2 of the SAS System for Windows (Copyright 2002-2008 SAS Institute Inc. SAS and all other SAS Institute Inc. product or service names are registered trademarks or trademarks of SAS Institute Inc., Cary, NC, USA).

Chapter 3 – Results

Hydrology

Mesocosm residence times for each experiment day were calculated from the injection flow rates and bromide breakthrough curve data. Residence times were surprisingly long for these short path lengths. The longest mean travel time was in MO on day 1 where it took 110 min for bromide to reach the 8.0 cm port. Mean travel times for the first 1.5 cm were relatively consistent between open-bottom mesocosms. For depths of 3.0 cm to 8.0 cm, day 1 residence times were much different than day 2 (Table 3). Day 1 had a mean travel time to 3.0 cm of 33 minutes and 49 minutes MO. Day 2 had a mean travel time to 3.0 cm of 64 minutes and 31 minutes in MO. Once mesocosms were cleaned on day 3, flow rates to each port in each MO were almost identical. The largest differences in mean travel times for day 3 were to the depths of 3.0 cm and 8.0 cm. MO had a mean travel time of 10 minutes and 13 minutes to 3.0 cm on day 3. The 8.0 cm port had a mean travel time of 43 minutes and 34 minutes in MO on day 3. MC-ac had the same residence time on day 3 as the 8.0 cm depth in one of the open-bottom mesocosms. This can be used to compare the biogeochemical differences between surface storage and subsurface storage areas. Mean travel times and residence times are summarized in Table 3.

Table 3: Travel times for each mesocosm calculated from the bromide breakthrough curves. Residence time, T_r, was calculated using the equation $T_r = V_m/Q_{out}$ where V_m is the water volume in the mesocosm (mL) and Q_{out} is the volumetric flow rate out of the mesocosm (mL/min).

	Mean travel time (minutes)						Residence time (minutes)				
Mesocosm	Day 1	Day 1	Day 2	Day 2	Day 3	Depth (cm)	Day 1	Day 1	Day 2	Day 2	Day 3
MO	0	0	0	0	n.a.	0.0	330	330	330	330	n.a.
	9	10	14	21	n.a.	1.5	339	340	344	351	n.a.
	33	49	64	31	n.a.	3.0	363	379	394	361	n.a.
	50	82	64	46	n.a.	5.0	380	412	394	376	n.a.
	n.a	110	96	90	n.a.	8.0	n.a.	440	426	420	n.a.
MO-c	n.a.	n.a.	n.a.	n.a.	0	0.0	n.a.	n.a.	n.a.	n.a.	340
	n.a.	n.a.	n.a.	n.a.	2	1.5	n.a.	n.a.	n.a.	n.a.	342
	n.a.	n.a.	n.a.	n.a.	13	3.0	n.a.	n.a.	n.a.	n.a.	353
	n.a.	n.a.	n.a.	n.a.	20	5.0	n.a.	n.a.	n.a.	n.a.	360
	n.a.	n.a.	n.a.	n.a.	34	8.0	n.a.	n.a.	n.a.	n.a.	374
MO-ac	n.a.	n.a.	n.a.	n.a.	0	0.0	n.a.	n.a.	n.a.	n.a.	340
	n.a.	n.a.	n.a.	n.a.	2	1.5	n.a.	n.a.	n.a.	n.a.	342
	n.a.	n.a.	n.a.	n.a.	10	3.0	n.a.	n.a.	n.a.	n.a.	350
	n.a.	n.a.	n.a.	n.a.	20	5.0	n.a.	n.a.	n.a.	n.a.	360
	n.a.	n.a.	n.a.	n.a.	43	8.0	n.a.	n.a.	n.a.	n.a.	383
MC	0	n.a.	0	n.a.	n.a.	0.0	362	n.a.	378	n.a.	n.a.
MC-ac	n.a.	n.a.	n.a.	n.a.	0	0.0	n.a.	n.a.	n.a.	n.a.	374

n.a. denotes not applicable.

Day vs. Night

MO, MO-c, and MC were compared to determine what different processes occurred during daylight hours versus night hours. Linear regression models of the cumulative mass loads from the inlet and outlet were used to determine whether NO_x, PO_4^{3-}, NH_4^+, TDN, and DOC increased or decreased through the subsurface flowpath. Analysis of the injectate showed the composition remained consistent for each mesocosm throughout the day and between each experiment. Therefore, all changes in concentration were due to processes within the mesocosms. A decrease in cumulative mass load from inlet to outlet would show retention occurred. DON values were either zero or minimal enough to be assumed no DON was present. TDN was then considered an

unnecessary analyte since its fluctuations were reflected in the NO_x and NH_4^+ results. A summary of the nutrient concentration ranges can be found in Table 4 while regression results can be found in Table 5.

Table 4: Nutrient concentration ranges for each mesocosm.

Mesocosm	DOC-C range (mg/L)	NO_x-N range (mg/L)	NH_4^+-N range (µg/L)	PO_4^{3-}-P range (µg/L)
MO	1.22-8.69	1.00-6.22	0.00-38.00	0.00-101.95
MO-c	1.35-4.21	1.61-6.22	0.00-24.00	4.73-95.48
MO-ac	1.77-8.22	2.45-6.37	0.00-32.00	5.25-108.29
MC	2.15-4.69	2.84-6.28	0.00-24.00	12.19-113.13
MC-ac	1.39-4.04	1.42-6.34	0.00-34.00	19.51-116.49
Overall	**1.22-8.69**	**1.00-6.37**	**0.00-38.00**	**0.00-116.49**

Table 5: **The rate of retention of the analyte from the inlet (sediment-water interface) to the outlet (8.0 cm depth) determined from linear regression models. Retention has a negative rate value while a gain in the analyte has a positive rate value.**

Mesocosm	DOC-C rate (mg/min)	Standard Error	NO_x-N rate (mg/min)	Standard Error	NH_4^+-N rate (µg/min)	Standard Error	PO_4^{3-}-P rate (µg/min)	Standard Error
MO***	0.011	± 0.0025	-0.040	± 0.0026	-0.66	± 0.034	-0.66	± 0.078
MO-c***	-0.012	± 0.0027	-0.061	± 0.0033	-0.89	± 0.022	0.24	± 0.068
MO-ac***	-0.088	± 0.0083	-0.073	± 0.0024	-1.22	± 0.018	-2.21	± 0.11
MC***	0.012	± 0.0019	-0.018	± 0.0049	0.36	± 0.073	0.50	± 0.11
MC-ac***	-0.011	± 0.0011	-0.018	± 0.0028	0.32	± 0.024	0.32	± 0.081

***Statistical significance of 0.001

Diurnal curves were seen in the continuous pH and DO saturation data for MO (Figure 4a, Figure 4b). Each began to increase at 7:00 with temperature and pH peaking between 15:00 and 16:00 each day (approximately 240-300 min into the experiment). DO within MO and MC peaked at 15:00 (240 min into the experiment) on day 1 and at 12:00 (60 min into the experiment) on day 2. Once the biota was cleaned on day 3, DO within MO-c increased from

7:00 to 9:00 where it plateaued before decreasing at 20:00 (approximately 540 min into the experiment) (Figure 4a). DO started out undersaturated within MO but soon became supersaturated (Figure 4a). MO had a peak value of 126.1% while MC was never supersaturated, its peak value being 97.7%. Point YSI data showed MO-c maintained undersaturated conditions throughout the day (~62%).

a)

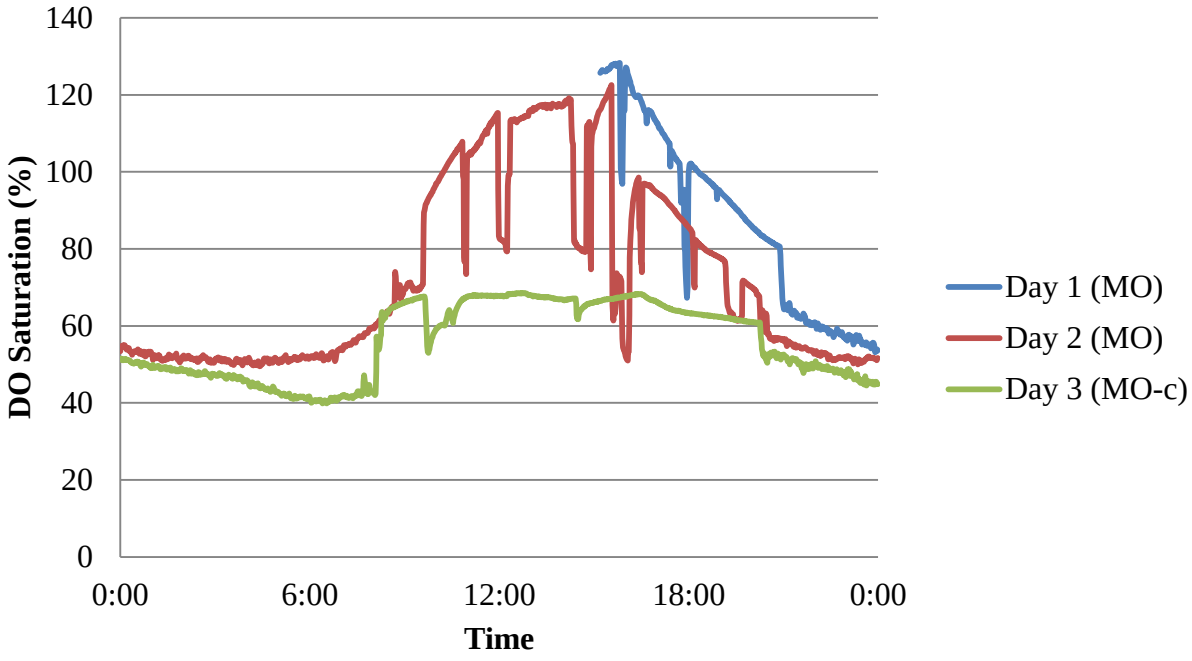

b)

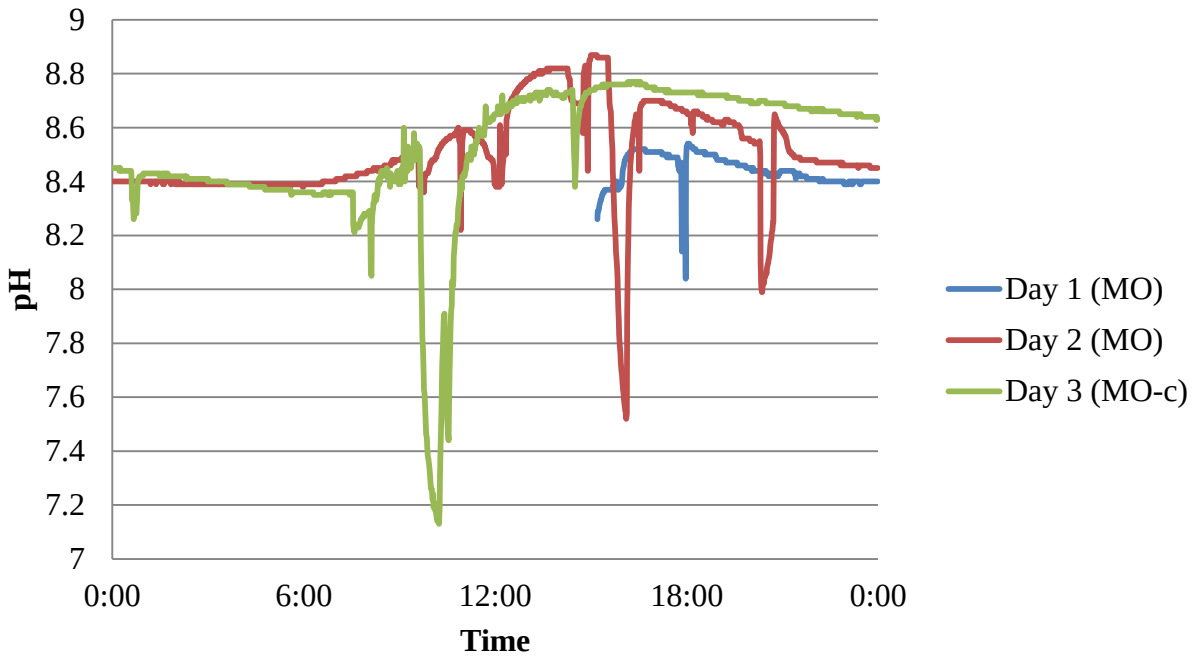

Figure 4: Dissolved oxygen saturation (a) and pH data (b) for MO and MO-c from YSI multiprobe continuous data.

MO and MC had similar DOC patterns throughout the experiment. Upon cleaning, DOC retention within MO-c changed dramatically. MO and MC showed an overall gain in DOC (Figure 5 and Figure 6 respectively) while MO-c showed clear retention of DOC (Figure 7). DOC exhibited a diurnal response within MO as indicated by the cumulative mass load regression (Figure 5). DOC concentrations within MO were similar at the inlet and outlet during daylight hours. At 19:00 (400 minutes into the experiment), MO exhibited a sudden gain in DOC at the outlet. MC gained DOC but the rate throughout the day did not change (Figure 6).

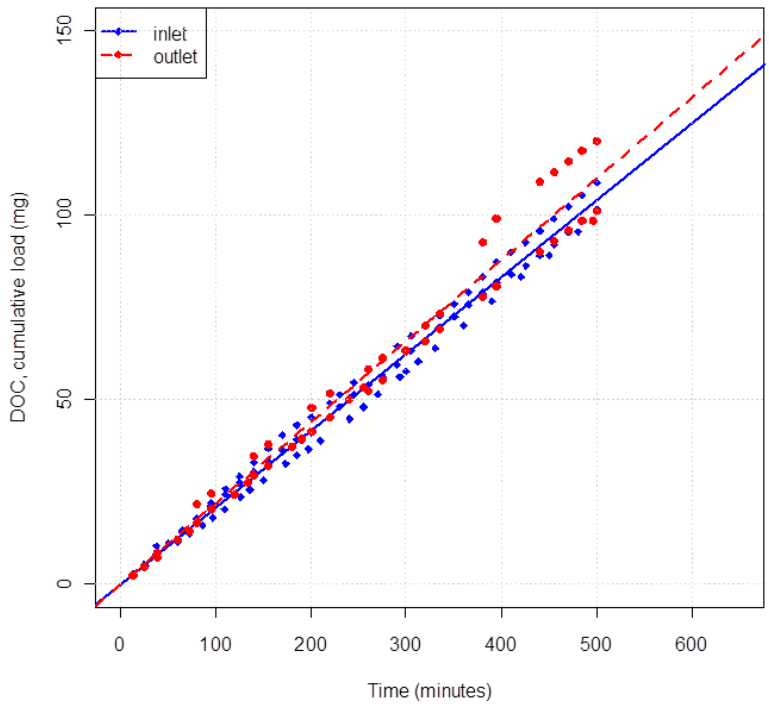

Figure 5: Linear regression data (dots) and model (lines) for the cumulative mass load of dissolved organic carbon within the open-bottom mesocosms. Time is the time passed (in minutes) since the start of the experiment.

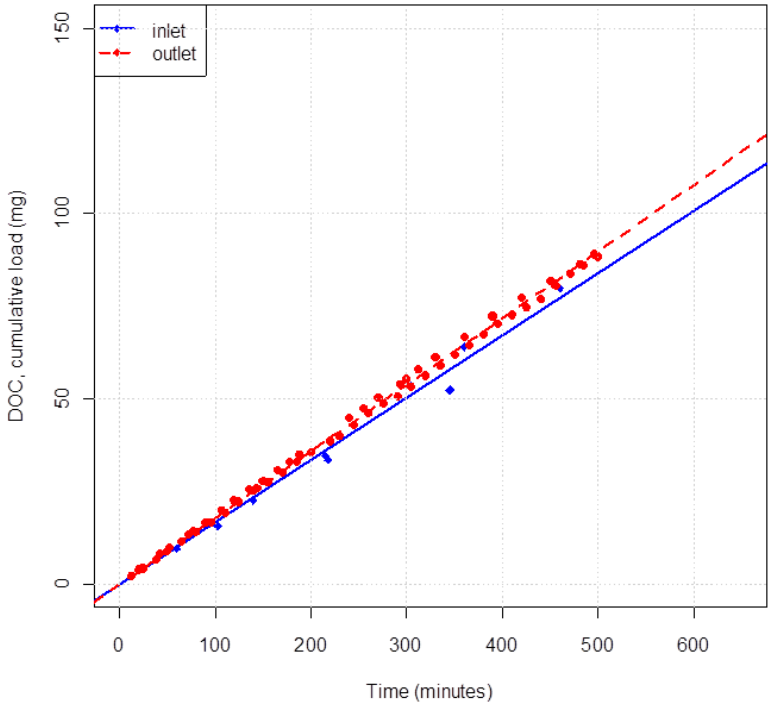

Figure 6: Linear regression data (dots) and model (lines) for the cumulative mass load of dissolved organic carbon within the closed-bottom mesocosms. Time is the time passed (in minutes) since the start of the experiment.

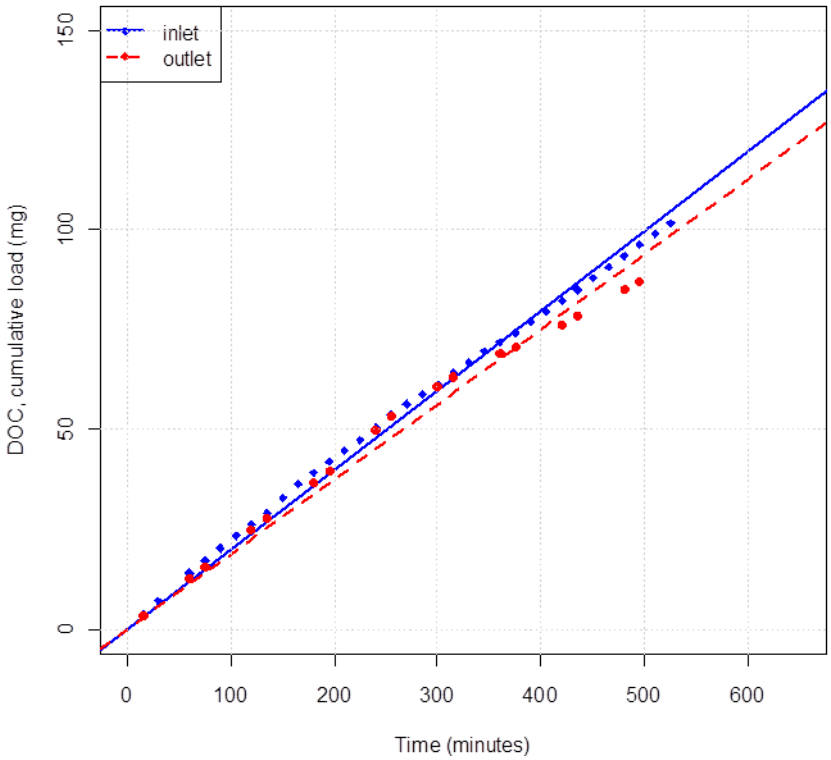

Figure 7: Linear regression data (dots) and model (lines) for the cumulative mass load of dissolved organic carbon within the open-bottom mesocosm after cleaning. Time is the time passed (in minutes) since the start of the experiment.

MO had opposing PO_4^{3-} patterns to MC and MO-c. MO had retention of PO_4^{3-} on each experiment day while MC had a strong gain in PO_4^{3-} each day. Upon cleaning, MO-c showed a gain in PO_4^{3-} at about half the rate of MC. There was, like DOC, a diurnal curve within the cumulative mass load for MO, MC, and MO-c. The diurnal curve showed increased rates started around 100 minutes and ended around 350 minutes into the experiment. These times correspond to 13:55 and 18:05 respectively.

Nitrogen species also exhibited contrasting patterns within MO, MO-c, and MC. Within MO and MO-c, NO_x and NH_4^+ exhibited diurnal curves where retention at the inlet increased around 100 minutes (13:55) and then decreased around 350 minutes into the experiment (18:05). MO had very consistent NO_x retention rates each day, while MC had about half the NO_x retention

rate as MO. MO-c had slightly higher nitrogen retention rates than MO. MC always gained NH_4^+, while MO and MO-c always had complete retention of NH_4^+. MC did have diurnal curves for nitrogen similar to MO and MO-c. The NH_4^+ and NO_x rates within MC still increased and decreased at approximately 13:55 and 18:05 respectively.

PARAFAC analysis can determine the percentage of DOM related to thirteen known fluorescing moieties [*Cory and McKnight*, 2005]. Similar fluorescing abilities indicate comparable properties exist which allows for the characterization of DOM. There were also statistically significant differences in PARAFAC components with time, depth, and mesocosm. The PARAFAC model determined Q3, a component related to microbial precursor material, appeared within MO-c between the depths of 1.5 and 5.0 cm between the hours of 14:30 and 19:30. HQ, also associated with microbial precursors, increased between the inlet and 3.0 cm of MO-c. The surface waters of MO-c showed a diurnal curve for HQ/Q2 values (a ratio comparing the dominance of terrestrial, Q2, versus microbial, HQ, material) with the peak occurring at 15:30 (Figure 8). Q1, related to terrestrial material, appeared only twice, once in the beginning hour of the experiment and once in the last hour of the experiment. SQ1 and Q2, both related to terrestrial precursors, had fairly consistent values throughout the day at approximately 20% and 15% respectively. HQ/Q2 depth profiles for MO-c varied heavily with no clear pattern. The outlet of the open-bottom mesocosms had significantly higher SUVA values than the inlet ($p = 0.027$). SUVA values were also significantly different with time ($p = 0.0002$). Time 18:30 had higher SUVA values than times 13:15, 14:30, and 15:30 within the surface waters. In the subsurface waters, SUVA was significantly higher at 12:30 and 18:30 than times 13:15, 14:30, and 15:30.

PARAFAC results for MC-ac had a much more consistent pattern throughout the day. DOM composition maintained the same characteristics throughout the day with only slight variations occurring with the SQ1 and HQ components. SQ1 (terrestrial) increased slightly during the night hours of 19:30 and 20:30 while HQ (microbial) decreased at the night hours of 20:30. The surface waters of MC-ac and MO-c did not have significantly different SUVA, FI, or protein values. MC-ac did have significantly lower SUVA values between the daylight hours of 13:15 and 15:30 than the evening hours after 18:30.

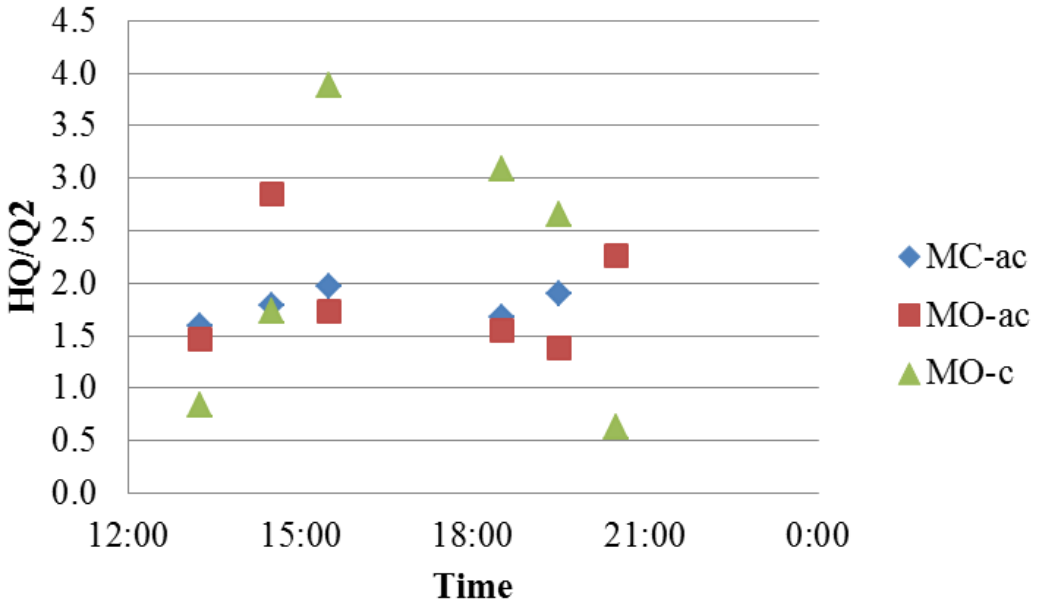

Figure 8: **HQ/Q2 ratios for the surface water of MO-ac, MO-c, and MC-ac.**

Sediment-water Interface

Nutrient profiles for MO and MO-c (Figure 9 and Figure 10 respectively) were compared to MC in order to examine how nutrients changed traveling from the surface water into and along subsurface flow paths. Nutrient profiles were examined during daylight hours (100 minutes from the start of the experiment) and night hours (600 minutes after the start of the experiment). The MO profile showed a gradual DOC increase occurred with depth which aligns with the gain in

DOC as indicated by the cumulative mass load. MC and MO showed similar gains in DOC at a rate of 0.011 and 0.012 mg/min respectively (Table 5). In contrast, MO-c had a gradual decrease in DOC concentrations with depth which aligns with the retention indicated by the cumulative mass load.

PO_4^{3-} profiles for MO and MO-c were very similar for both the day and night profiles (Figure 9 and Figure 10 respectively). PO_4^{3-} decreased sharply between the surface waters and a depth of 1.5 cm in MO and MO-c. From a depth of 1.5 cm to 8.0 cm, PO_4^{3-} consistently increased with depth until the outlet within MO-c and MO. MO-c had greater subsurface concentrations at the outlet than surface water concentrations. In contrast, MO had greater concentrations at the outlet. This was also indicated in the cumulative mass load because MO retained PO_4^{3-} while MO-c gained PO_4^{3-}. With the sediment-water interface absent, MC also gained PO_4^{3-}. MO-c gained PO_4^{3-} at half the rate of MC.

Nitrogen species were transformed very differently along subsurface paths. NO_x concentrations only had small variations when traveling from the surface water through the subsurface. NO_x did consistently decrease within MO and MO-c from the surface to a depth of 1.5 cm (Figure 9 and Figure 10 respectively). There was very little variation after 1.5 cm so this small distance caused the overall retention of NO_x as determined by the cumulative mass load. In the absence of the sediment-water interface, MC had only slight NO_x retention at a rate of 0.018 mg/min (Table 5). Profiles for NH_4^+ were identical for MO and MO-c (Figure 9 and Figure 10 respectively). NH_4^+ was completely removed between the inlet and 1.5 cm and it did not return at depth. In contrast, MC gained NH_4^+ at a rate of 0.40 µg/min (Table 5).

a)

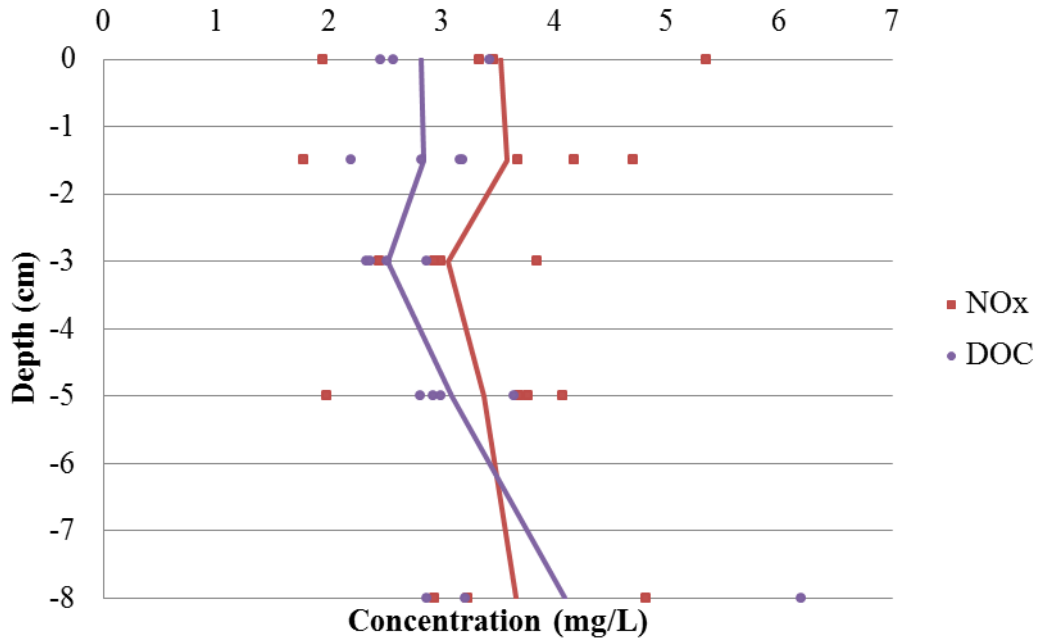
0
1
2
3
4
5
6
7
0
-1
-2
-3
-4
-5
-6
-7
-8
Depth (cm)
Concentration (mg/L)
NOx
DOC

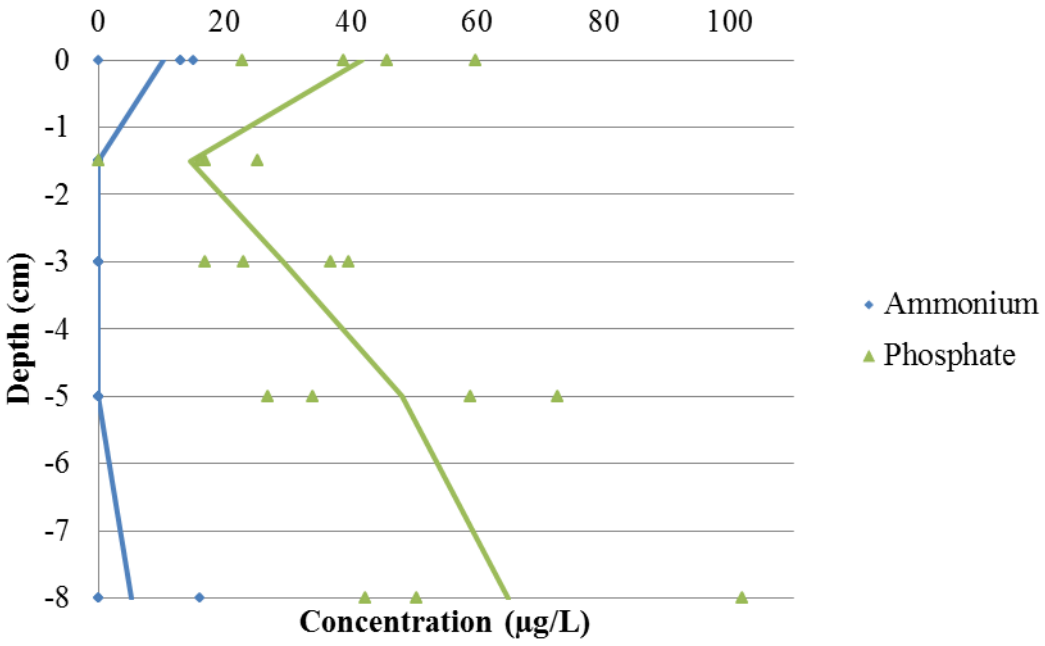
0
20
40
60
80
100
0
-1
-2
-3
-4
-5
-6
-7
-8
Depth (cm)
Concentration (µg/L)
Ammonium
Phosphate

b)

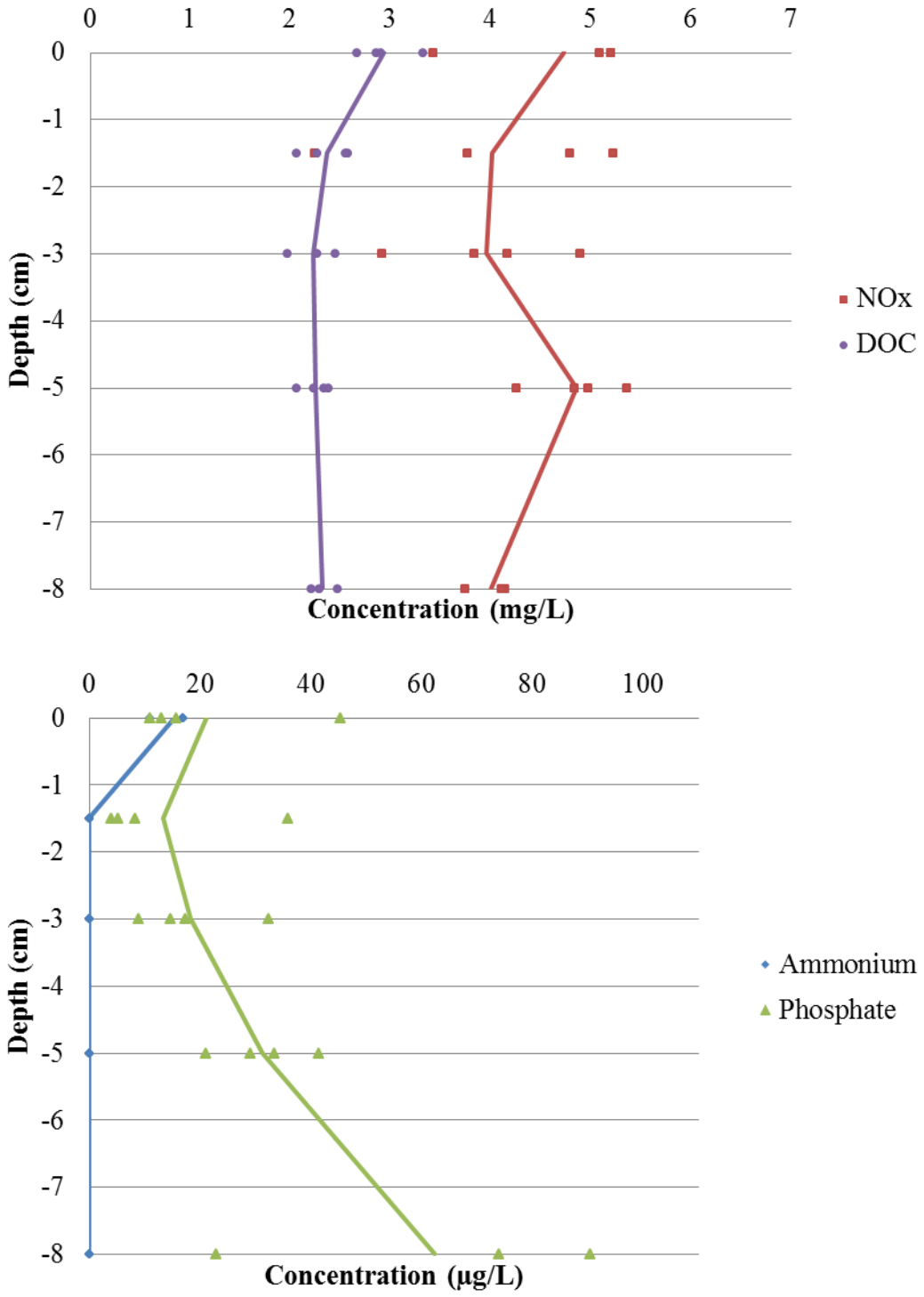

Figure 9: Profiles for DOC, NO_x, NH_4^+, and PO_4^{3-} within the open-bottom mesocosm (MO) during the day (a) and night (b).

a)

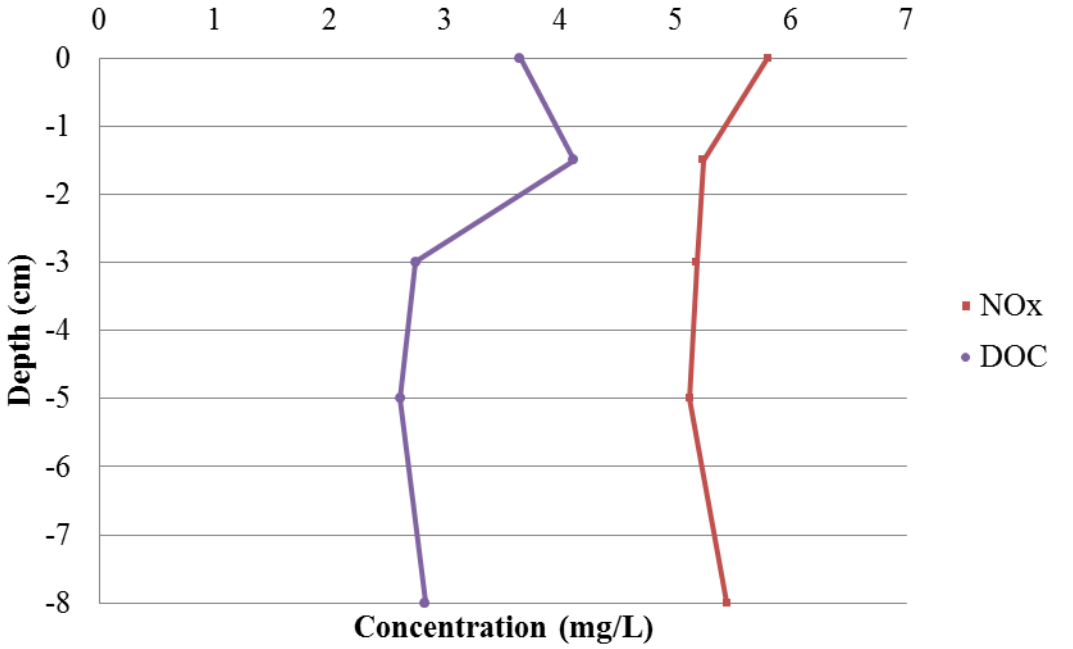
0
1
2
3
4
5
6
7
0
-1
-2
-3
-4
-5
-6
-7
-8
Depth (cm)
Concentration (mg/L)
NOx
DOC

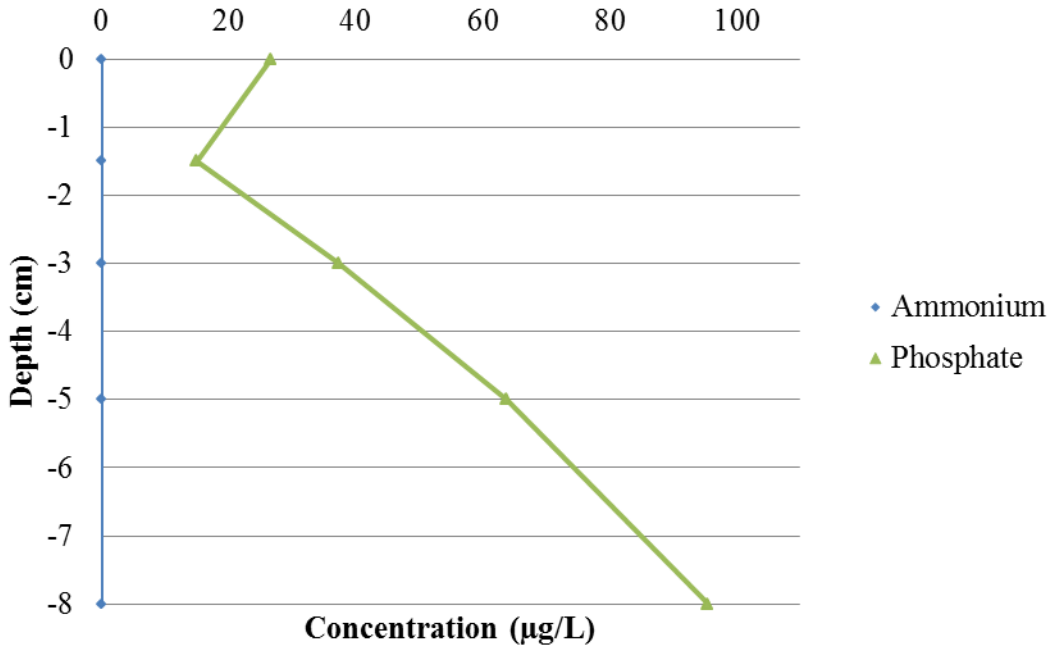
0
20
40
60
80
100
0
-1
-2
-3
-4
-5
-6
-7
-8
Depth (cm)
Concentration (µg/L)
Ammonium
Phosphate

b)

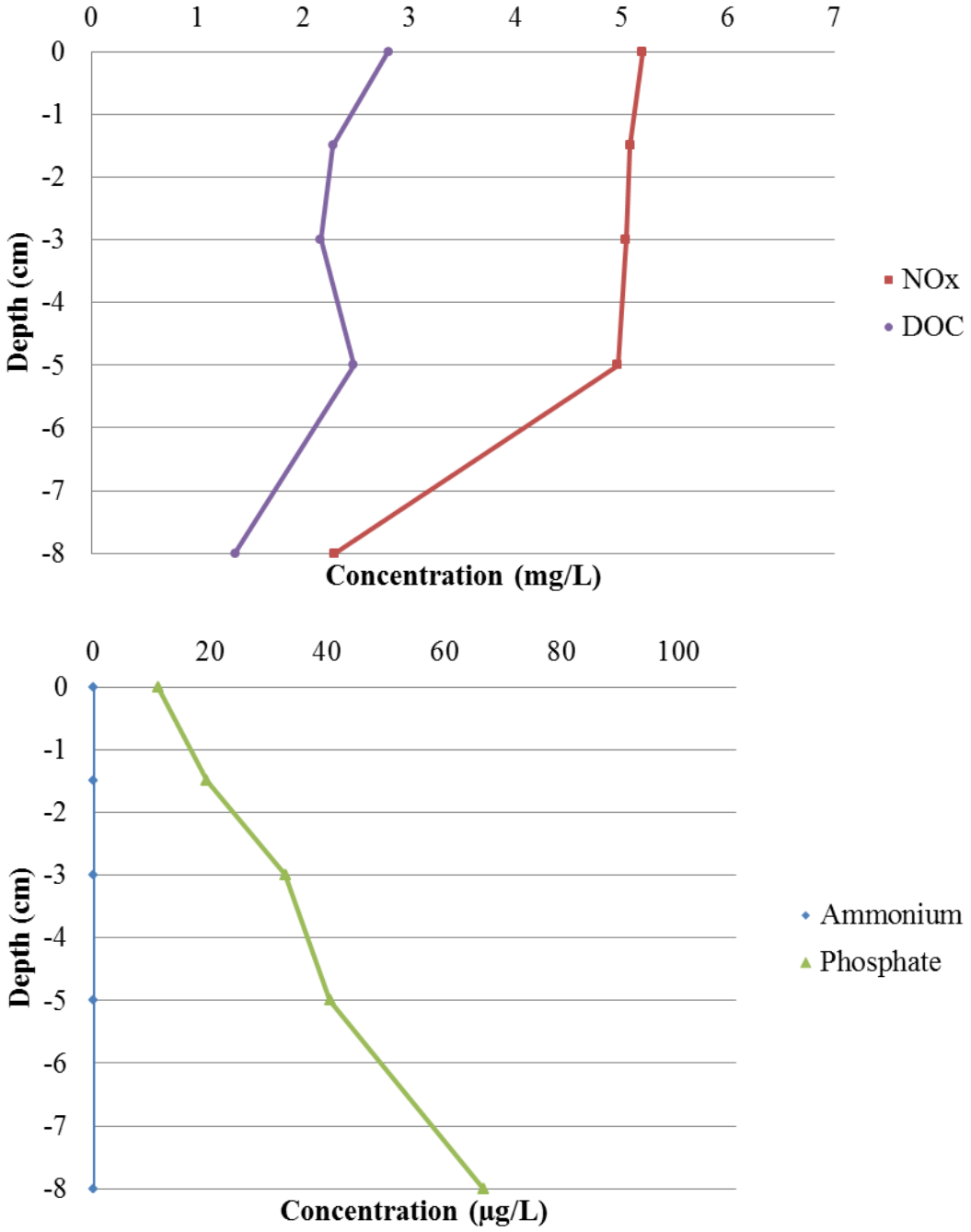

Figure 10: **Profiles for DOC, NO_x, NH_4^+, and PO_4^{3-} within the open-bottom mesocosm (MO-c) after cleaning during the day (a) and night (b).**

Acidification

Nutrient profiles and DOM analysis from MO-ac were compared to MO and MO-c to determine the impact of acidification. YSI profiles of pH were taken using point measurements of water withdrawn from each depth. MO-ac pH profiles for 17:52 and 20:15 were almost identical with pH values of 6.9, 7.3, 7.4, 7.4, and 7.5 measured for the depths 0, 1.5, 3.0, 5.0, and 8.0 cm respectively.

a)

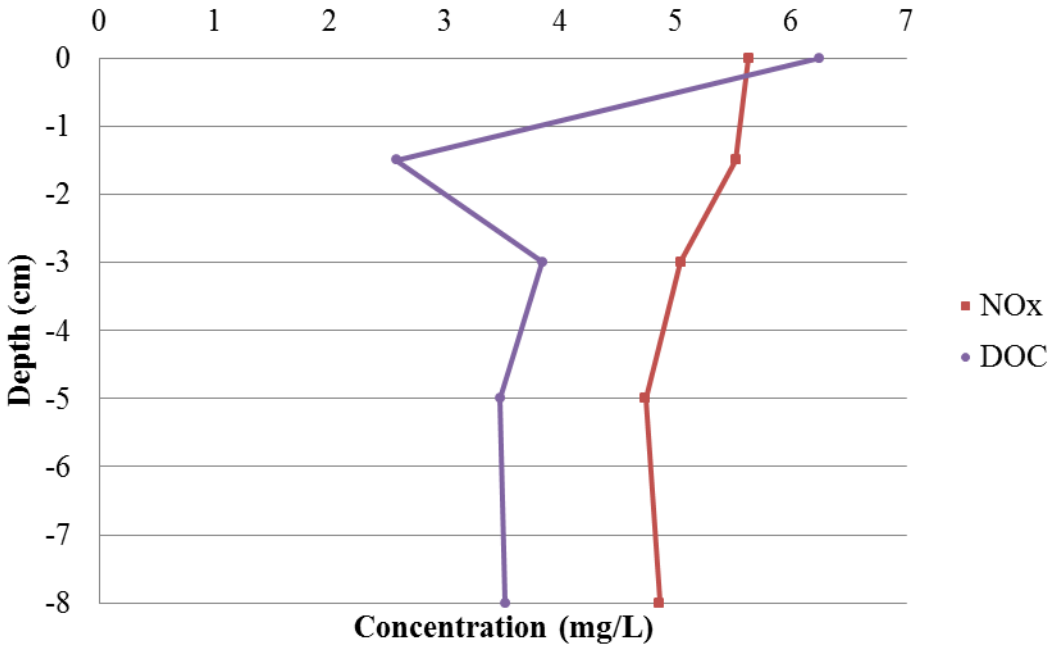

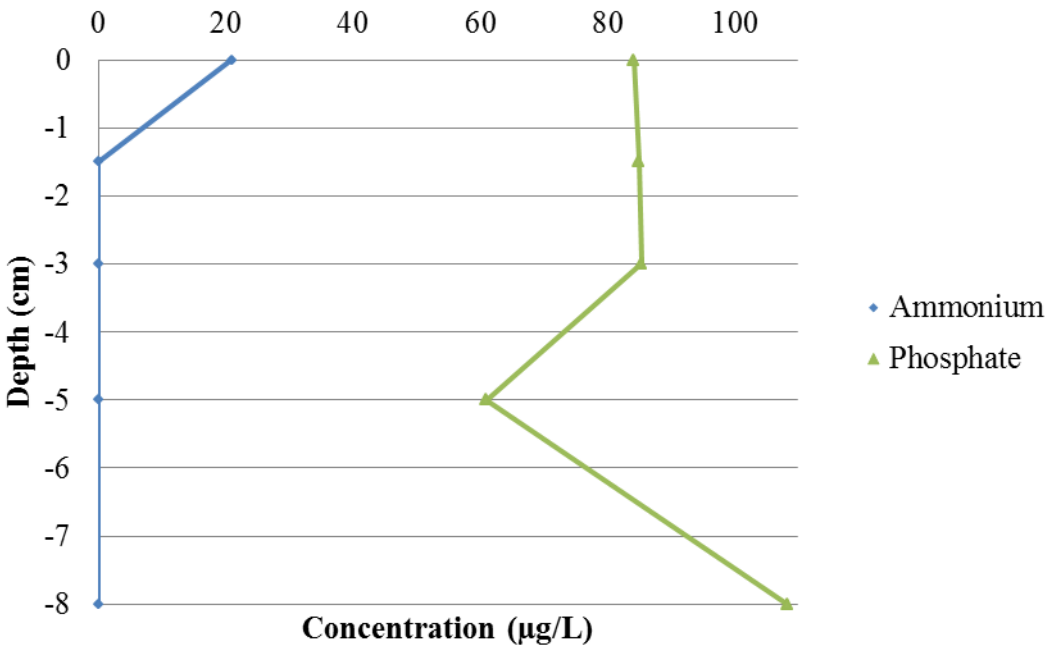
0
20
40
60
80
100
0
-1
-2
-3
-4
-5
-6
-7
-8
Depth (cm)
Concentration (µg/L)
Ammonium
Phosphate

b)

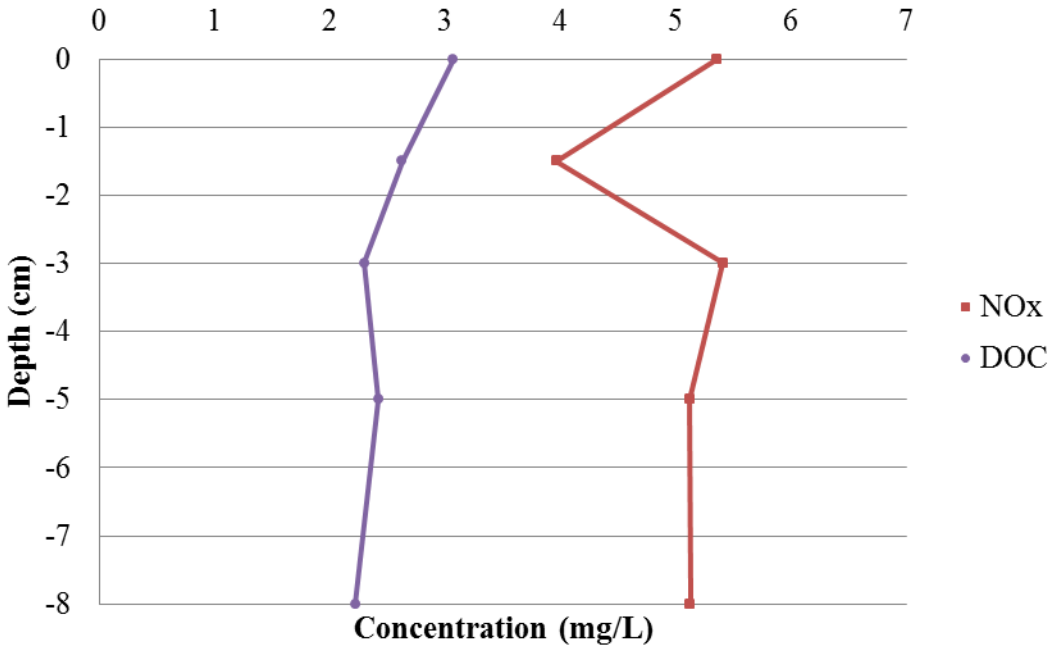
0
1
2
3
4
5
6
7
0
-1
-2
-3
-4
-5
-6
-7
-8
Depth (cm)
Concentration (mg/L)
NOx
DOC

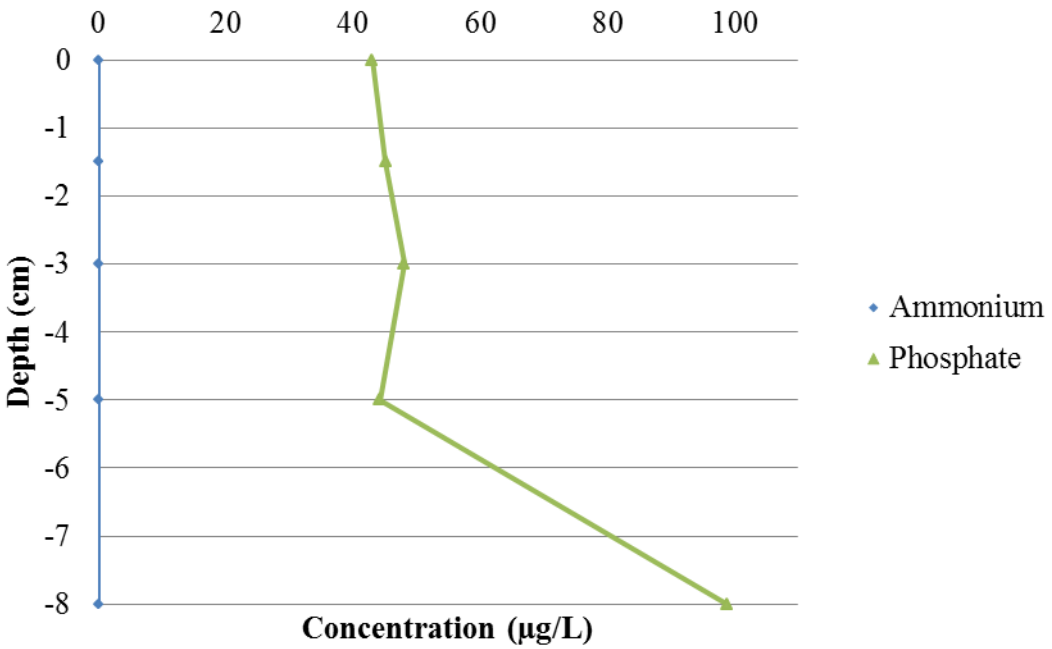

Figure 11: Profiles for DOC, NO_x, NH_4^+, and PO_4^{3-} within the open-bottom mesocosm after cleaning and acidification (MO-ac) during the day (a) and night (b).

Acidification greatly affected DOC concentrations within the surface water. The MO-ac profile and cumulative mass load showed inlet DOC concentrations were much higher than MO and MO-c (Figure 5-7). MO-ac, like normal pH conditions, exhibited a decrease in concentration between the inlet and a depth of 1.5 cm (Figure 11). Subsurface concentrations of DOC were then similar to concentrations for typical pH conditions (Figure 9-11). This increased retention in MO-ac between the surface and 1.5 cm was indicated in the cumulative mass load with a higher DOC retention rate (-0.088 mg/min as C) than MO-c (-0.012 mg/min as C) (Table 5). Under normal pH conditions before cleaning, MO exhibited an increase in DOC (Table 5). When removing the sediment-water interface, MC-ac had a DOC retention rate of -0.011 mg/min as C while MC had a gain in DOC (0.012 mg/min as C) (Table 5).

Under normal pH conditions, MO had a sharp decrease in PO_4^{3-} concentrations between the inlet and a depth of 1.5 cm (Figure 9). In contrast, the depth profile for acidified conditions

showed concentrations remained constant in MO-ac from the inlet to a depth of about 3-5 cm before increasing at the outlet (Figure 11). MO-ac also had a higher retention rate (2.21 µg/min as P) than MO (0.58 µg/min as P) (Table 5). Like DOC, the MO-ac profile showed higher inlet concentrations than MO but these values returned to concentrations similar to MO as seen in the night profile. Without the sediment-water interface, MC-a had a slightly lower rate of PO_4^{3-} gain (0.32 µg/min as P) than MC (0.50 µg/min as P) (Table 5).

Nutrient profiles for NO_x and NH_4^+ did not change significantly between acidified and unacidified conditions. MC-ac and MC had exactly the same NO_x retention rate (-0.018 mg/min as N) (Table 5). MO and MO-ac had different NO_x retention rates (0.040 mg/min as N and 0.073 mg/min as N respectively), but this is most likely due to the removal of biota since MO-ac and MO-c have similar retention rates (0.073 mg/min as N and 0.061 mg/min as N respectively) (Table 5). Acidification also had no impact on the rate of NH_4^+ gain within MC-a and MC (0.32 µg/min as P and 0.50 µg/min as P respectively) (Table 5). There was always complete retention of NH_4^+ in any open-bottom mesocosm but acidification caused MO-ac to have about twice the NH_4^+ retention rate as MO (1.22 µg/min as N and 0.66 µg/min as N respectively) (Table 5). The cumulative mass load showed, like DOC and PO_4^{3-}, inlet concentrations were slightly higher for MO-ac than MO which caused this increased retention.

Since acidification influenced DOC retention, DOM characterization was also impacted. MO-ac had significantly higher protein content than MO-c within the surface water ($p = 0.048$) and within the subsurface water ($p = 0.006$) on day 3. The surface water protein content of MO-ac and MO-c were not significantly different than MC-a. HQ/Q2 within the surface water of MO-ac was very similar to MC-a (Figure 8).

The time-mesocosm interaction was significant for surface water RI values ($p = 0.035$). The specific significant differences could not be determined because there were no replicates for this higher order interaction. Within the subsurface water, RI was significant for mesocosm ($p = 0.030$) and the time-depth interaction ($p = 0.038$). Analysis in SAS, however, showed RI and time was also significant ($p = 0.012$). MO-ac was more reduced (had higher RI values) than MO-c. Time 14:30 was more oxidized than times 13:15 and 20:30. The specific differences for the time-depth interaction could not be determined since there were no replicates for this higher order interaction.

The pH change did impact SUVA values but not FI. FI was not significant within the surface or subsurface waters while SUVA was significant with time ($p = 0.037$) and mesocosm ($p = 0.051$) in the surface water. Within the surface water, MO-c had higher (more terrestrial) SUVA values than MO-ac. Time 18:30 had higher SUVA values than times 13:15, 14:30, and 15:30. Within the subsurface, SUVA was significant with time ($p = 0$), depth ($p = 0.001$), and mesocosm ($p = 0.002$). MO-ac had higher SUVA values than MO-c. As DOM passed from the surface to the subsurface, SUVA values at the outlet became significantly higher than the inlet. Times 18:30 and 20:30 had higher SUVA values than times 13:15, 14:30, and 15:30.

Chapter 4 – Discussion

Day vs. Night

Photosynthesis by the autotrophic community was clearly occurring throughout the experiment due to clear diurnal DO, pH, and nutrient (NH_4^+, NO_x, PO_4^{3-}) curves. DO also becomes supersaturated which can only occur when photosynthesis is taking place. DO peaked at 126.1% around 15:00. DO and pH then returned to baseline values throughout the night. DO increases during photosynthesis due to the oxygen production and pH decreases due to uptake of

CO_2 from the water column. Once biota was removed, DO levels within MO-c remained undersaturated which further supports photosynthesis being a vital process.

There was a clear change in the rate DOC was gained starting approximately 370 minutes into the experiment (approximately 17:00) as seen in the cumulative mass load (Figure 5). At that point, DOC concentrations started increasing at the outlet. The injection concentration did not change so a physical or chemical process within the mesocosm must have changed. The physical conditions of the mesocosm were being controlled so chemical changes, as YSI data confirmed, occurred as photosynthesis shut off around 15:00. The increase at the outlet could therefore be due to phototrophs dying off once photosynthesis ended. MO-c also had a diurnal curve present in the cumulative mass load but MO-c had DOC retention throughout the day, even after photosynthesis stopped. The autotrophic community was very subdued within MO-c as seen with the muted diurnal DO curve. Without an active autotrophic community, DOC was not produced so MO-c would not gain DOC. Retention of DOC, however, could occur due to sorption to the sediment.

PO_4^{3-}, NH_4^+, and NO_x also showed diurnal curves within the regressions for cumulative mass load of MO. Rate changes for each nutrient occurred at the same time (13:55 and 18:05) which also corresponded to pH, DO, and temperature peaks recorded with the YSI suggesting the nutrients were retained via assimilation. The same diurnal pattern occurred for NH_4^+ within MC except NH_4^+ had an overall gain possibly due to photochemical oxidation.

The impact of photosynthesis on nutrient retention was also seen in DOM quality. Nutrient retention was observed in the profiles at 1.5 cm and Q3 (microbial) also appeared at the depths of 1.5 to 5.0 cm during photosynthetic hours (14:30 to 19:30) [*Cory and McKnight*, 2005]. HQ (microbial) also increased between the inlet and 1.5 cm. The highest peak of HQ in MO within

surface waters occurred at 14:30 (180 minutes into the experiment) which again corresponded to the photosynthesis peak. There was a clear diurnal curve for HQ/Q2 in the surface water of MO-c (Figure 8). This curve corresponds to peak daylight hours which clearly points to the DOM quality changing to microbially derived DOM during the day and more terrestrially derived at night. Q1 (terrestrial) only appears in the first and last hours of the experiment which further supports the change of DOM quality. The percentage of SQ1 and Q2 (both terrestrial) present throughout the day remained constant so the terrestrial input was not changing. The microbial input was changing so in-situ production is most likely occurring. Miller et al [2009a] showed microbial fulvic acids are produced during biotic growth so these microbial signals are evidence there was microbial growth or algal exudates occurring during daylight hours. Depth profiles of HQ/Q2 for MO-c are heavily varied which could be due to the fluctuations of DOM flushing.

Statistical analysis of the PARAFAC components showed MO-ac and MO-c had significant differences in protein content. MO-ac had higher protein content within the surface and subsurface waters. This along with MO-ac having lower SUVA values than MO-c is evidence MO-ac had more microbial precursors. Acidification and cleaning, however, took away the photosynthetic response within MO-ac. DO saturation of MC-ac and MO-ac were both ~62% throughout day 3 and there was no diurnal HQ/Q2 response. It has been shown photochemical oxidation will decrease the SUVA value [*Brooks et al.*, 2007]. Miller et al. [2009a] showed microbially-derived fulvic acid can look like it is being produced when photolysis of non-humic DOM occurs. New DOM was being produced by microbes and microbial uptake of DOM was occurring simultaneously with photochemical DOM transformations so it is hard to differentiate the role of photolysis in altering DOM chemical quality. With microbial activity in MO-ac removed (as seen by the muted pH and DO peak), the decreased SUVA value and increased

protein signal in MO-ac give strong evidence of the photochemical impact on DOM composition.

Since there was strong evidence for photosynthesis and photochemical oxidation occurring at the inlet, there should be a larger microbial signal at the inlet. The outlet of the open-bottom mesocosms had significantly higher (more terrestrial) SUVA values than the inlet which supports the inlet having microbial dominance. The change in SUVA with time also reflects the impact of photosynthesis and photochemical oxidation on carbon quality. Once the sunlight stops hitting the mesocosm (18:30), the SUVA value is significantly higher (mean > 2.0, more terrestrial) than peak photosynthesis hours (13:15, 14:30, and 15:30) (mean < 2.0, more microbial). This corresponds to photosynthetic activity stopping at night. The subsurface also reflected these time differences with samples from 18:30 and 20:30 having more terrestrial SUVA values than the peak photosynthetic times of 13:15, 14:30, and 15:30. The strong biological activity occurring within the surface waters shows the sediment-water interface is very important for nutrient retention.

Sediment-water Interface

The cumulative mass load analysis showed an overall gain in DOC within MO. Depth profiles, however, showed DOC decreased from the surface water to a depth of 1.5 cm which is similar to other studies [*Baker et al.*, 1999]. PO_4^{3-}, NH_4^+, and NO_x decreased from the inlet to a depth of 1.5 cm. DO, pH, and DOM analysis proved photosynthesis was occurring within the mesocosms and this was further confirmed by the nutrient retention that occurred across the sediment-water interface.

NH_4^+ is more favorable than NO_x for mineralization because the bond energy within NH_4^+ requires less energy to break and utilize N than it does for NO_x. Results suggest mineralization

was prevalent since NH_4^+ was always used up completely. The demand for N was therefore greater than the supply so organisms turned to using NO_x. Depth profiles showed NO_x concentrations only decreased from the inlet to a depth of 1.5 cm (Figure 9-10). The incorporation of NO_x onto suspended material is not an important NO_x sink [*Bohlke et al.*, 2004] so nutrient retention due to mineralization is supported. There was also no significant change seen in NO_x concentrations within MC which further supports the sediment-water interface is important for denitrification and uptake.

The importance of the sediment-water interface for nutrient retention was reinforced by the NH_4^+ profile and comparison to MC. NH_4^+ was completely removed from the system each day as it crossed the sediment-water interface within the open-bottom mesocosms. MC, however, always gained NH_4^+ likely due to photochemical oxidation. Biological demand was too high to see if NH_4^+ was produced within the open-bottom mesocosms, but photochemical oxidation may explain why MO-c did not have a gain in DOC despite autotrophic signals. The apparent increased retention of NH_4^+ within MO-c could then be due to photochemical oxidation increasing concentrations within the surface water. The retention rate for NO_x within MO and MO-c were very similar (0.040 mg/min as N versus 0.061 mg/min as N respectively) and could be the natural variation of the stream between days.

The removal of biota caused a clear response in PO_4^{3-}. MO had PO_4^{3-} retention while MO-c had a slight increase in PO_4^{3-} from inlet to outlet. The daytime nutrient profile for MO-c initially showed a decrease in PO_4^{3-} from the inlet to 1.5 cm while the night profile showed a consistent gain in PO_4^{3-} with depth. Removing the sediment-water interface also caused a gain in PO_4^{3-} within MC which again shows the importance of the sediment-water interface for nutrient retention. The gain in PO_4^{3-} within MC could be due to a similar mechanism as the NH_4^+ gain.

Photochemical oxidation of iron oxide contained within suspended particles can release attached PO_4^{3-}. The diurnal response of the inlet was not as clear for PO_4^{3-} as it was for NH_4^+, but evidence of a change in rate between peak daylight hours and evening hours was present and supports this theory.

Despite active nutrient retention from the surface water to a depth of 1.5 cm, depth profiles for MO and MO-c showed PO_4^{3-} increased with depth. This could be due to desorption or to the redox gradient causing reductive dissolution of Fe-hydroxides. There was no Fe^{2+} found at depth but the field instrument had questionable results so it is possible the instrument was malfunctioning and Fe^{2+} was present (unpublished data). RI values, however, did not have significant differences with depth so it is hard to determine exactly what caused the increase. PO_4^{3-} was, however, highly influenced by the presence or absence of biota, and the sediment-water interface had a major impact on PO_4^{3-} retention.

Acidification

Acidification caused DOC at the sediment-water interface to be desorbed, increasing surface water concentrations. Acidification may have also caused the release of DOC from sediment particles within MC because inlet concentrations increased but outlet concentrations were similar to MC (Figure 5-7). The increased retention of DOC throughout the day suggests DOC was eventually resorbed. The release of sediment DOM within MC-ac and MO-ac were not significantly different which further supports the DOM was not from a microbial source. Although MO-ac was impacted by acidification, photosynthesis was still occurring since SUVA values in the evening (18:30) were significantly different than peak photosynthesis hours (13:15, 14:30, 15:30).

NO_x regression analysis showed acidification had no impact on retention as observed by the consistent retention rates across mesocosms. Since NO_x retention remains the same, denitrifiers were apparently unaffected by acidification. Similarly, NH_4^+ was unaffected by acidification since it was still completely retained. MC-ac also continued to have photooxidation creating NH_4^+ at the same rate as unacidified conditions.

Acidification did have an effect on PO_4^{3-} retention. Like NH_4^+, acidification released PO_4^{3-} from the sediment into the water column. Although the increased presence of PO_4^{3--} led to higher retention rates, PO_4^{3-} concentrations increased at the outlet. Therefore, acidification caused an overall decrease in PO_4^{3-} retention. MC-ac also showed a higher inlet and outlet concentration. Acidification of MC-ac released PO_4^{3-} from suspended particles while retention processes remained unchanged. Since outlet concentrations ultimately increased, the retention efficiency decreased which is similar to other studies [*Mulholland et al.*, 2008].

The diurnal response of inlet PO_4^{3-} concentrations within MC-ac were much less pronounced than MC. This increase could be due to acidification releasing PO_4^{3-} attached to iron oxides. The redox gradient in MO-ac was impacted by acidification so iron reducing microorganisms could be present, causing the release of PO_4^{3-}. Acidification and cleaning interfered with the autotrophic community as seen by the muted HQ/Q2 diurnal curve (Figure 8). MO-ac still shows some autotrophic impact with HQ/Q2 having some diurnal response but it was not like the pronounced MO-c data.

Chapter 5 – Summary and Conclusions

These results quantify the nutrient retention occurring at the sediment-water interface which is vital when trying to understand in-stream nutrient processing for management purposes. These results showed photosynthetic activity caused N and PO_4^{3-} retention and a decrease in DOC. The

DOM quality was also changed from a more microbially derived DOM during the day to a more terrestrially derived DOM at night due to the autotrophic community producing DOC. An acute acidification event caused a decreased response of the autotrophic community. Acidification also caused a decrease in the efficiency of PO_4^{3-} retention because more PO_4^{3-} was released from the sediment than could be retained by biota and sorption. Acidification also impacted DOM characterization because DOC was released from the sediment.

These results are important to study because the physical and chemical structure of streams will change as climate change threatens to bring unstable environmental conditions. Climate change could bring less frequent but more intense storms which would remove the active biotic community at the sediment-water interface. The impacts of climate change are unknown but these results suggest if stream acidification events were to increase, the biotic community, and therefore nutrient retention, would be reduced while inputs of PO_4^{3-} increase as it is released from the sediment. Future work should study the nutrient processing occurring along upwelling zones under the same conditions. Together, downwelling and upwelling results can be used to quantify total stream nutrient retention based on an estimate of the surface area they cover along a stream. These results can be used to develop more effective management plans for the climate of today and, hopefully, the climate of tomorrow.

References

Alexander, R. B., R. A. Smith, and G. E. Schwarz (2000), Effect of stream channel size on the delivery of nitrogen to the Gulf of Mexico, *Nature*, *403*(6771), 758-761.

Baker, M. A., C. N. Dahm, and H. M. Valett (1999), Acetate retention and metabolism in the hyporheic zone of a mountain stream, *Limnol Oceanogr*, *44*(6), 1530-1539.

Bohlke, J. K., J. W. Harvey, and M. A. Voytek (2004), Reach-scale isotope tracer experiment to quantify denitrification and related processes in a nitrate-rich stream, midcontinent United States, *Limnol Oceanogr*, *49*(3), 821-838.

Brooks, M. L., J. S. Meyer, and D. M. McKnight (2007), Photooxidation of wetland and riverine dissolved organic matter: altered copper complexation and organic composition, *Hydrobiologia, 579*, 95-113.

Brown, A., D. M. McKnight, Y. P. Chin, E. C. Roberts, and M. Uhle (2004), Chemical characterization of dissolved organic material in Pony Lake, a saline coastal pond in Antarctica, *Mar Chem*, *89*(1-4), 327-337.

Carmichael, W. W. (2001), Health effects of toxin-producing cyanobacteria: "The CyanoHABs", *Hum Ecol Risk Assess*, *7*(5), 1393-1407.

Cory, R. M., and D. M. McKnight (2005), Fluorescence spectroscopy reveals ubiquitous presence of oxidized and reduced quinones in dissolved organic matter, *Environ Sci Technol, 39*(21), 8142-8149.

Cory, R. M., M. P. Miller, D. M. McKnight, J. J. Guerard, and P. L. Miller (2010), Effect of instrument-specific response on the analysis of fulvic acid fluorescence spectra, *Limnol Oceanogr-Meth*, *8*, 67-78.

Diaz, R. J., and R. Rosenberg (1995), Marine benthic hypoxia: A review of its ecological effects and the behavioral responses of benthic macrofauna, *Oceanography and Marine Biology Annual Review, 33*, 245-303.

Diaz, R. J., and R. Rosenberg (2008), Spreading dead zones and consequences for marine ecosystems, *Science, 321*(5891), 926-929.

Dingman, S. L. (2002), *Physical Hydrology*, 2nd ed., Prentice Hall.

Dodds, W. K., W. W. Bouska, J. L. Eitzmann, T. J. Pilger, K. L. Pitts, A. J. Riley, J. T. Schloesser, and D. J. Thornbrugh (2009), Eutrophication of US Freshwaters: Analysis of Potential Economic Damages, *Environ Sci Technol*, *43*(1), 12-19.

Dubrovsky, N. M., and P. A. Hamilton (2010), Nutrients in the Nation's streams and groundwater: National Findings and Implications: U.S., in *Geological Survey Fact Sheet 2010-3078*, edited.

Duff, J. H., F. Murphy, C. C. Fuller, F. J. Triska, J. W. Harvey, and A. P. Jackman (1998), A mini drivepoint sampler for measuring pore water solute concentrations in the hyporheic zone of sand-bottom streams, *Limnol Oceanogr*, *43*(6), 1378-1383.

Fellman, J. B., E. Hood, and R. G. M. Spencer (2010), Fluorescence spectroscopy opens new windows into dissolved organic matter dynamics in freshwater ecosystems: A review, *Limnol Oceanogr, 55*(6), 2452-2462.

Fellman, J. B., M. P. Miller, R. M. Cory, D. V. D'Amore, and D. White (2009), Characterizing Dissolved Organic Matter Using PARAFAC Modeling of Fluorescence Spectroscopy: A Comparison of Two Models, *Environ Sci Technol, 43*(16), 6228-6234.

Fredrick, B. S., J. I. Linard, J. L. Carpenter, National Water-Quality Assessment Program (U.S.), USGS Nebraska Water Science Center., and Geological Survey (U.S.) (2006), Environmental setting of Maple Creek watershed, Nebraska, in *Scientific investigations report 2006-5037*, edited, U.S. Geological Survey, Reston, Va.

Fuhrer, G. J., National Water-Quality Assessment Program (U.S.), and Geological Survey (U.S.) (1999), *The quality of our nation's waters : nutrients and pesticides*, 82 p. pp., U.S. Dept. of the Interior USGS Information Services [distributor], Reston, Va. Denver, CO.

Galloway, J. N., A. R. Townsend, J. W. Erisman, M. Bekunda, Z. Cai, J. R. Freney, L. A. Martinelli, S. P. Seitzinger, and M. A. Sutton (2008), Transformation of the Nitrogen Cycle: Recent Trends, Questions, and Potential Solutions, *Science, 320*, 889-892.

Green, S. A., and N. V. Blough (1994), Optical-Absorption and Fluorescence Properties of Chromophoric Dissolved Organic-Matter in Natural-Waters, *Limnol Oceanogr, 39*(8), 1903-1916.

Hawkins, P. R., M. T. C. Runnegar, A. R. B. Jackson, and I. R. Falconer (1985), Severe Hepatotoxicity Caused by the Tropical Cyanobacterium (Blue-Green-Alga) Cylindrospermopsis-Raciborskii (Woloszynska) Seenaya and Subba Raju Isolated from a Domestic Water-Supply Reservoir, *Appl Environ Microb, 50*(5), 1292-1295.

Hedin, L. O., J. C. von Fischer, N. E. Ostrom, B. P. Kennedy, M. G. Brown, and G. P. Robertson (1998), Thermodynamic constraints on nitrogen transformations and other biogeochemical processes at soil-stream interfaces, *Ecology, 79*(2), 684-703.

Jaffe, R., D. McKnight, N. Maie, R. Cory, W. H. McDowell, and J. L. Campbell (2008), Spatial and temporal variations in DOM composition in ecosystems: The importance of long-term monitoring of optical properties, *J Geophys Res-Biogeo, 113*(G4), -.

Keil, R. G., and D. L. Kirchman (1991), Contribution of Dissolved Free Amino-Acids and Ammonium to the Nitrogen Requirements of Heterotrophic Bacterioplankton, *Mar Ecol-Prog Ser, 73*(1), 1-10.

McKnight, D. M., E. W. Boyer, P. K. Westerhoff, P. T. Doran, T. Kulbe, and D. T. Andersen (2001), Spectrofluorometric characterization of dissolved organic matter for indication of precursor organic material and aromaticity, *Limnol Oceanogr, 46*(1), 38-48.

Mee, L. (2006), Reviving dead zones, *Sci Am, 295*(5), 78-85.

Mermillod-Blondin, F., L. Mauclaire, and B. Montuelle (2005), Use of slow filtration columns to assess oxygen respiration, consumption of dissolved organic carbon, nitrogen transformations. and microbial parameters in hyporheic sediments, *Water Res*, *39*(9), 1687-1698.

Miller, M. P., D. M. McKnight, and S. C. Chapra (2009a), Production of microbially-derived fulvic acid from photolysis of quinone-containing extracellular products of phytoplankton, *Aquat Sci*, *71*(2), 170-178.

Miller, M. P., D. M. McKnight, S. C. Chapra, and M. W. Williams (2009b), A model of degradation and production of three pools of dissolved organic matter in an alpine lake, *Limnol Oceanogr*, *54*(6), 2213-2227.

Miller, M. P., D. M. McKnight, R. M. Cory, M. W. Williams, and R. L. Runkel (2006), Hyporheic exchange and fulvic acid redox reactions in an alpine stream/wetland ecosystem, Colorado front range, *Environ Sci Technol*, *40*(19), 5943-5949.

Moore, M. V., M. L. Pace, J. R. Mather, P. S. Murdoch, R. W. Howarth, C. L. Folt, C. Y. Chen, H. F. Hemond, P. A. Flebbe, and C. T. Driscoll (1997), Potential effects of climate change on freshwater ecosystems of the New England/Mid-Atlantic Region, *Hydrol Process*, *11*(8), 925-947.

Mulholland, P. J., S. A. Thomas, H. M. Valett, J. R. Webster, and J. Beaulieu (2006), Effects of light on NO3- uptake in small forested streams: diurnal and day-to-day variations, *J N Am Benthol Soc*, *25*(3), 583-595.

Mulholland, P. J., et al. (2008), Stream denitrification across biomes and its response to anthropogenic nitrate loading, *Nature*, *452*(7184), 202-U246.

Murdoch, P. S., and J. L. Stoddard (1992), The Role of Nitrate in the Acidification of Streams in the Catskill Mountains of New-York, *Water Resour Res*, *28*(10), 2707-2720.

Puckett, L. J., C. Zamora, H. Essaid, J. T. Wilson, H. M. Johnson, M. J. Brayton, and J. R. Vogel (2008), Transport and fate of nitrate at the ground-water/surface-water interface, *J Environ Qual*, *37*(3), 1034-1050.

Rabalais, N. N., R. E. Turner, and W. J. Wiseman (2001), Hypoxia in the Gulf of Mexico, *J Environ Qual*, *30*(2), 320-329.

Rabalais, N. N., R. E. Turner, B. K. Sen Gupta, E. Platon, and M. L. Parsons (2007a), Sediments tell the history of eutrophication and hypoxia in the Northern Gulf of Mexico, *Ecol Appl*, *17*(5), S129-S143.

Rabalais, N. N., R. E. Turner, B. K. Sen Gupta, D. F. Boesch, P. Chapman, and M. C. Murrell (2007b), Hypoxia in the northern Gulf of Mexico: Does the science support the plan to reduce, mitigate, and control hypoxia?, *Estuar Coast*, *30*(5), 753-772.

Sheibley, R. W., J. H. Duff, A. P. Jackman, and F. J. Triska (2003), Inorganic nitrogen transformations in the bed of the Shingobee River, Minnesota: Integrating hydrologic and biological processes using sediment perfusion cores, *Limnol Oceanogr*, *48*(3), 1129-1140.

Stedmon, C. A., S. Markager, and R. Bro (2003), Tracing dissolved organic matter in aquatic environments using a new approach to fluorescence spectroscopy, *Mar Chem*, *82*(3-4), 239-254.

Thouin, J. A., W. M. Wollheim, C. J. Vorosmarty, J. M. Jacobs, and W. H. McDowell (2009), The biogeochemical influences of NO3-, dissolved O-2, and dissolved organic C on stream NO3- uptake, *J N Am Benthol Soc*, *28*(4), 894-907.

Triska, F. J., V. C. Kennedy, R. J. Avanzino, G. W. Zellweger, and K. E. Bencala (1989), Retention and Transport of Nutrients in a 3rd-Order Stream in Northwestern California - Hyporheic Processes, *Ecology*, *70*(6), 1893-1905.

Turlan, T., F. Birgand, and P. Marmonier (2007), Comparative use of field and laboratory mesocosms for in-stream nitrate uptake measurement, *Ann Limnol-Int J Lim*, *43*(1), 41-51.

Weishaar, J. L., G. R. Aiken, B. A. Bergamaschi, M. S. Fram, R. Fujii, and K. Mopper (2003), Evaluation of specific ultraviolet absorbance as an indicator of the chemical composition and reactivity of dissolved organic carbon, *Environ Sci Technol*, *37*(20), 4702-4708.

Wetzel, R. G. (1992), Gradient-Dominated Ecosystems - Sources and Regulatory Functions of Dissolved Organic-Matter in Fresh-Water Ecosystems, *Hydrobiologia*, *229*, 181-198.

Appendix A: Methods and Data

A.1 Particle Size Analysis

Sediment cores taken from the field site were analyzed for particle size analysis using the AASHTO T27 Sieve Analysis of Fine and Coarse Aggregates. The results are presented below in Table A.1.1.

Table A.1.1: Particle size analysis for Maple Creek sediment cores.

Sieve #	Size (mm)	Percent Composition
4	>4.76	2.30
10	>2.00	4.66
16	>1.19	4.69
35	>0.500	26.32
50	>0.295	41.25
100	>0.149	17.84
200	>0.074	0.02
<200	≤0.074	2.92

A.2 Breakthrough Curves

The first two hours of the experiment had frequent sampling in order to develop bromide breakthrough curves. Hydraulic residence time was calculated based on the mean travel time for bromide to reach each sampling depth. Mean travel time was determined by the time it took for bromide to reach a concentration equal to half of the plateau concentration. Background bromide concentrations were accounted for when calculated the mean travel time. Residence times for the closed-bottom mesocosm were determined from the pumping rate. Bromide breakthrough curves for each open-bottom mesocosm are shown in Figures A.2.1 to A.2.6. Table A.2.1 summarizes the results for the mean travel times to each depth within each open-bottom mesocosm.

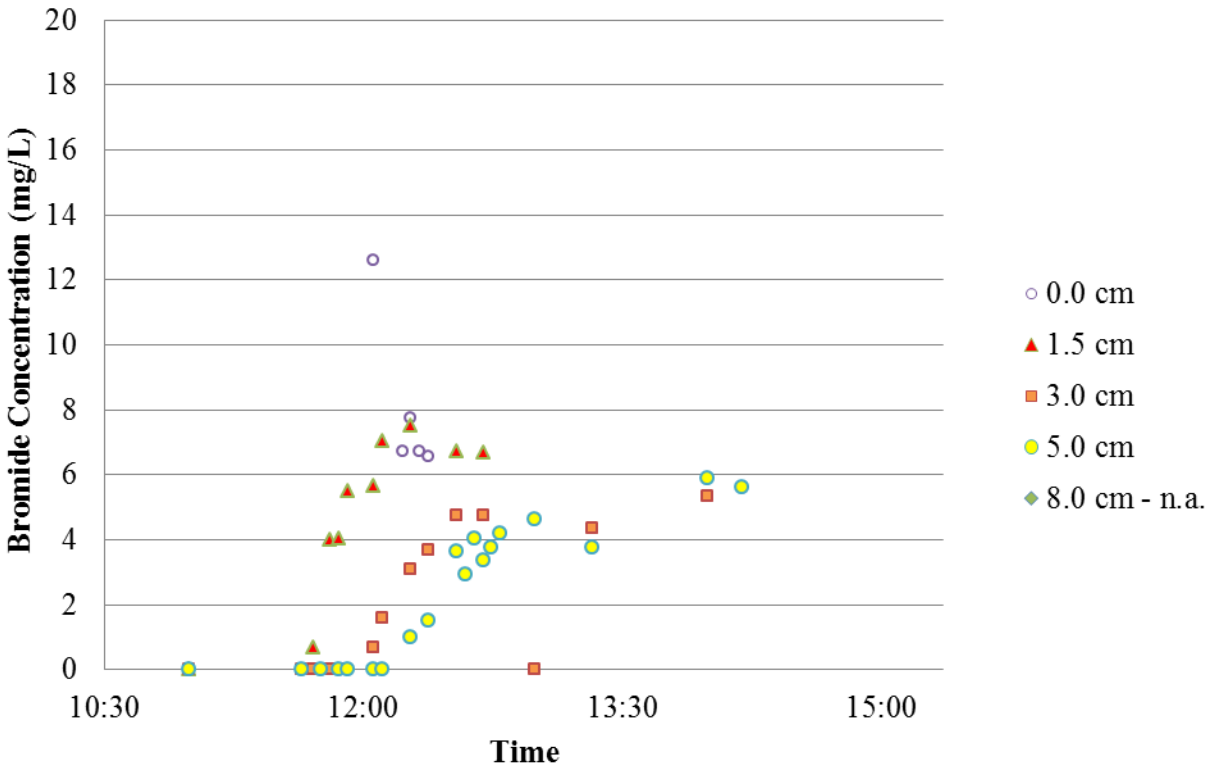

Figure A.2.1: Bromide breakthrough curves for MO replicate #1. n.a. denotes not available.

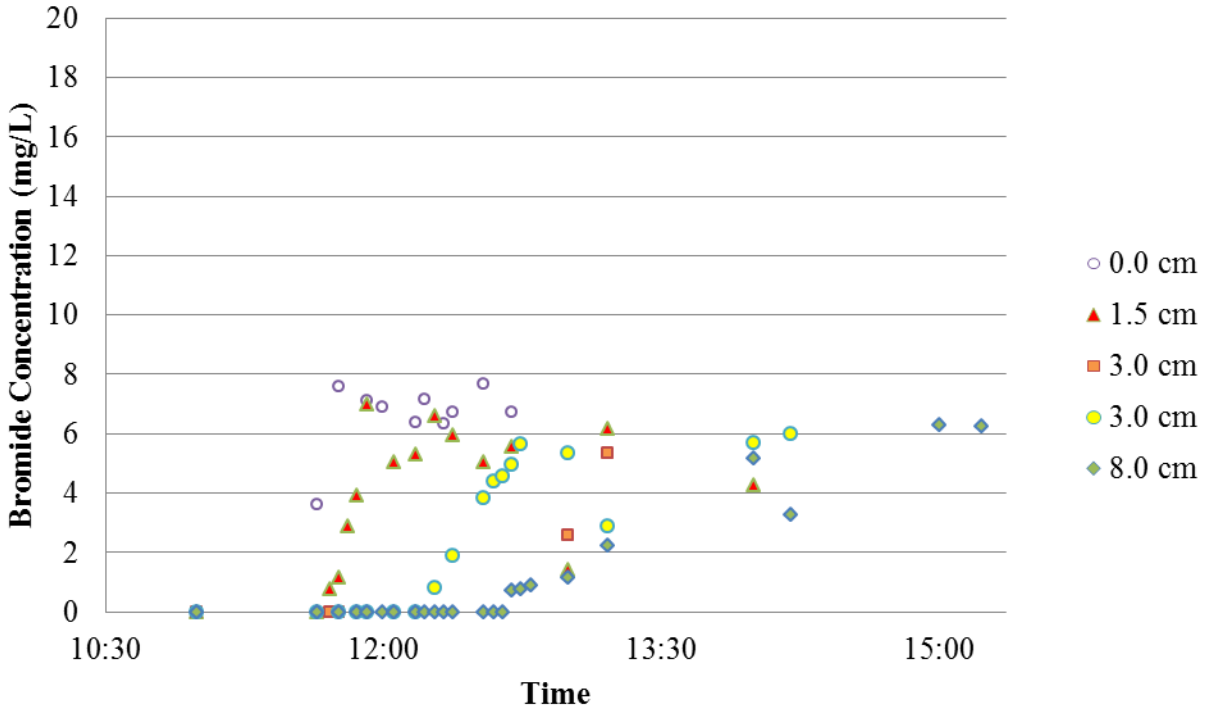

Figure A.2.2: Bromide breakthrough curves for MO replicate #2.

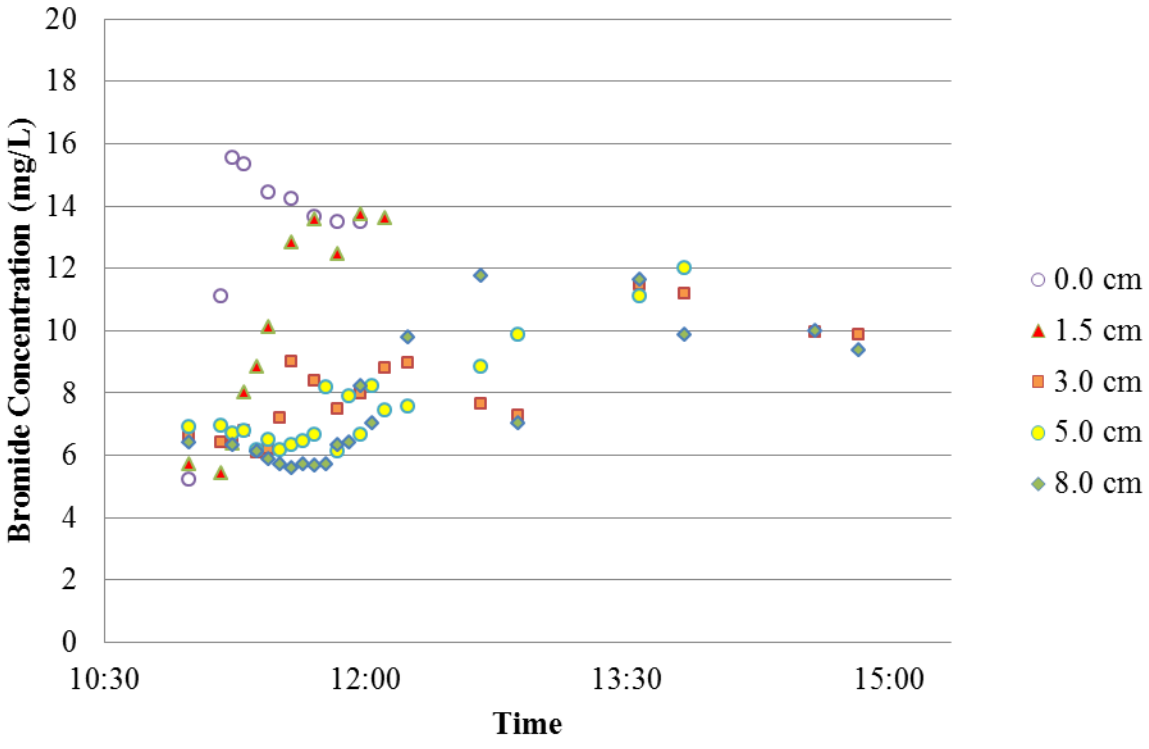

Figure A.2.3: Bromide breakthrough curves for MO replicate #3.

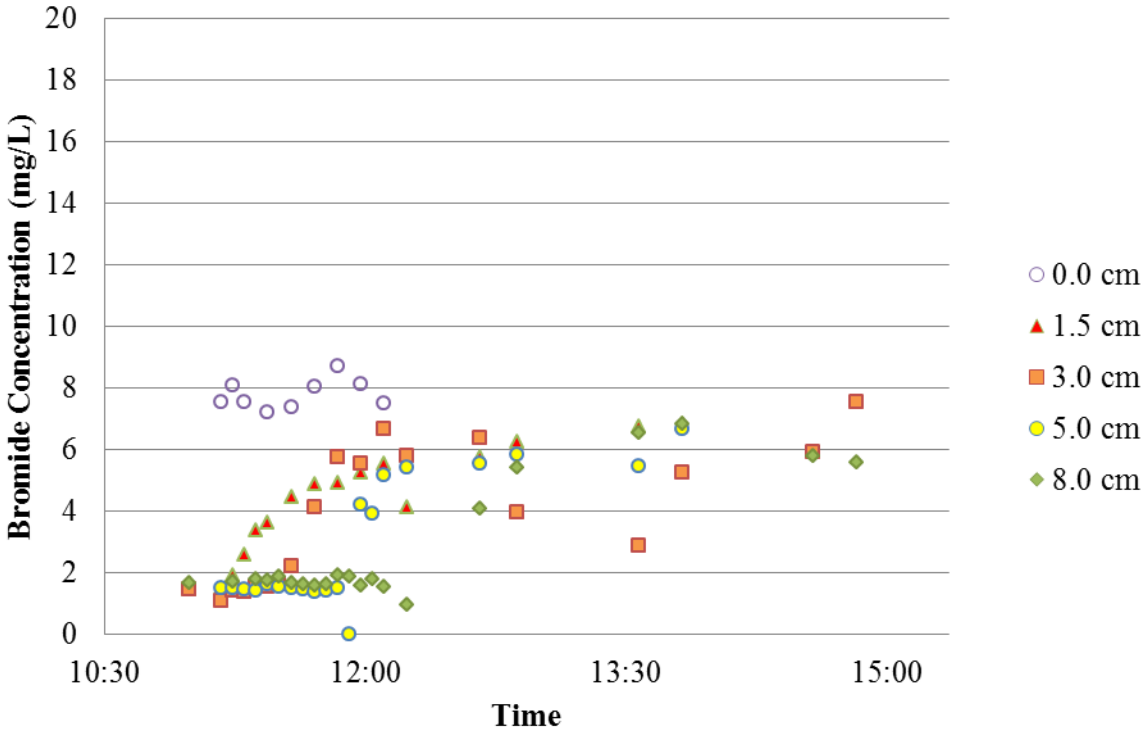

Figure A.2.4: Bromide breakthrough curves for MO replicate #4.

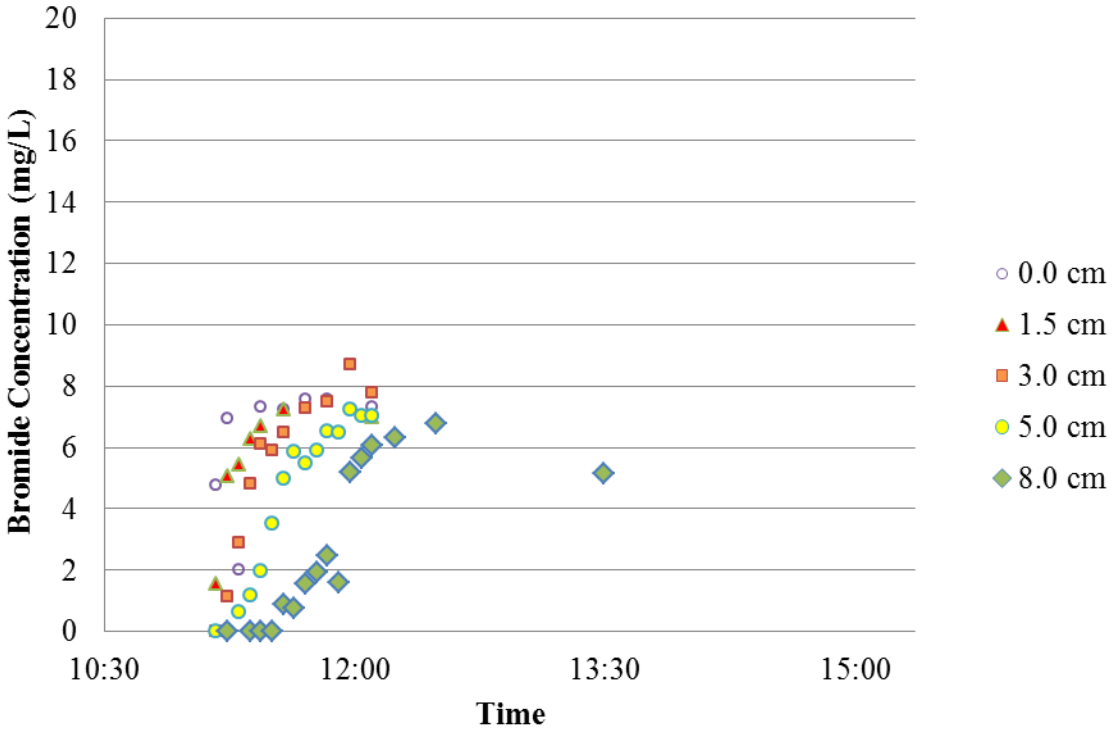

Figure A.2.5: Bromide breakthrough curves for MO-ac.

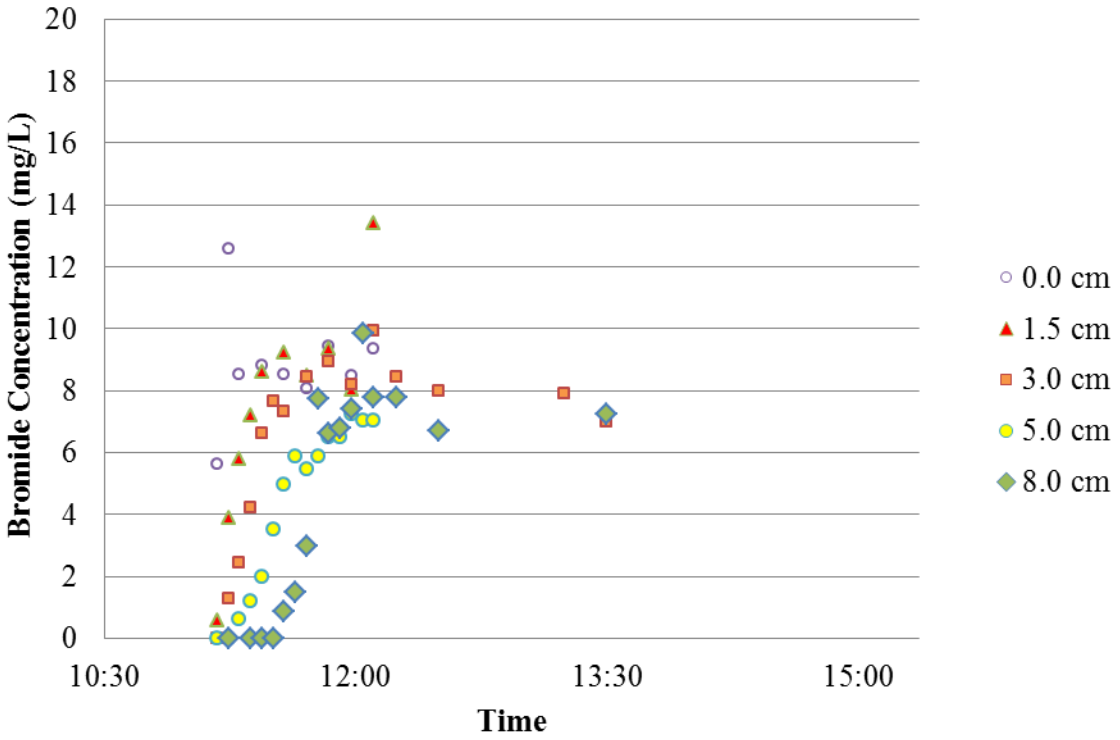

Figure A.2.6: Bromide breakthrough curves for MO-c

Table A.2.1: Mean travel times for each depth and mesocosm. Bromide concentrations are those after subtracting out any background signal. n.a. denotes not available.

Mesocosm	Depth (cm)	Time at start	Time at half concentration plateau	Br concentration at plateau (mg/L)	Br concentration at half of the plateau concentration (mg/L)	Mean Travel time (min)
MO	0	11:39	0:00	6.70	3.35	0
	1.5	11:39	11:48	6.70	3.35	9
	3	11:39	12:12	4.70	2.35	33
	5	11:39	12:29	5.00	2.50	50
	8	11:39	n.a.	n.a.	n.a.	n.a
MO	0	11:39	0:00	6.70	3.35	0
	1.5	11:39	11:49	6.00	3.00	10
	3	11:39	13:01	5.50	2.75	82
	5	11:39	12:28	5.67	2.83	49
	8	11:39	13:29	6.20	3.1	110
MO	0	11:11	11:11	13.60	9.42	0
	1.5	11:11	11:25	13.60	9.57	14
	3	11:11	12:15	11.20	8.88	64
	5	11:11	12:47	11.50	9.19	96

	8	11:11	12:15	10.00	8.22	64
MO	0	11:11	11:11	7.78	4.63	0
	1.5	11:11	11:32	6.78	4.11	21
	3	11:11	11:42	6.30	3.87	31
	5	11:11	11:57	6.00	3.75	46
	8	11:11	12:41	6.65	4.16	90
MO-ac	0	11:11	11:11	7.40	3.70	0
	1.5	11:11	11:13	7.20	3.60	2
	3	11:11	11:21	7.60	3.80	10
	5	11:11	11:31	7.00	3.50	20
	8	11:11	11:54	6.70	3.35	43
MO-c	0	11:11	11:11	8.70	4.35	0
	1.5	11:11	11:13	9.30	4.65	2
	3	11:11	11:24	9.90	4.95	13
	5	11:11	11:31	7.30	3.65	20
	8	11:11	11:45	7.77	3.885	34

A.3 Nutrient and DOC Data with Flow Rates

Table A.3.1 summarizes the nutrient and DOC data obtained over the course of this experiment. Background and injection concentrations for each constituent as well as flow rates for each mesocosm are also given.

Table A.3.1: Nutrient, DOC, and flow rate data for MO, MO-ac, MO-c, MC, and MC-ac. Injection samples are labeled as "inj" and background samples are labeled as "back". b.d. stands for "below detection" and n.a. denotes not available.

Time	Mesocosm	Depth	NH_4^+ - N (ug/L)	NO_3^- - N (mg/L)	PO_4^{3-} - P (ug/L)	DOC (mg/L)	TDN (mg/L)	Flow Rate (mL/min)
13:00	MC	0	0.000	5.224	90.933	3.073	5.243	62
13:20	MC	0	0.000	5.223	97.956	3.300	4.940	62
13:42	MC	0	18.000	4.381	54.295	2.876	3.850	62
13:52	MC	0	0.000	5.336	101.288	2.957	5.121	62
14:12	MC	0	0.000	4.721	88.694	2.768	4.427	62
14:18	MC	0	0.000	5.556	63.243	2.893	5.166	62
14:30	MC	0	0.000	5.613	53.638	3.202	5.176	62
14:45	MC	inj	0.000	6.281	12.758	2.412	4.457	62
14:47	MC	0	17.000	4.135	92.682	3.107	4.130	62
15:00	MC	0	10.000	5.479	28.997	3.092	5.270	62
15:16	MC	0	0.000	4.422	37.571	2.718	4.365	62
15:30	MC	0	16.000	5.089	35.950	2.848	4.614	62

15:45	MC	0	0.000	5.358	31.708	3.205	5.205	62
15:58	MC	0	0.000	3.224	33.824	2.691	2.873	62
16:08	MC	0	14.000	4.029	22.785	3.279	3.844	62
16:28	MC	inj	0.000	5.494	48.916	2.538	4.724	62
17:00	MC	0	0.000	5.347	68.304	2.839	4.976	62
17:15	MC	0	0.000	5.837	34.303	3.000	4.854	62
17:30	MC	0	12.000	5.333	70.439	3.036	5.082	62
17:53	MC	0	15.000	4.914	28.838	2.307	3.557	62
18:00	MC	0	17.000	4.935	85.870	3.417	4.830	62
18:12	MC	0	12.000	5.346	42.607	2.946	5.272	62
18:23	MC	inj	0.000	6.259	50.576	2.430	4.391	62
18:30	MC	0	11.000	5.192	49.705	2.938	5.154	62
19:00	MC	0	14.000	4.133	82.707	3.134	3.979	62
19:30	MC	0	14.000	5.497	23.716	2.877	4.866	62
20:00	MC	0	14.000	4.487	23.860	2.422	3.674	62
20:30	MC	0	0.000	5.505	38.006	2.600	4.886	62
20:30	MC	inj	0.000	5.228	36.303	2.360	4.403	62
21:00	MC	0	0.000	5.559	14.858	2.393	4.663	62
21:16	MC	0	14.000	3.803	12.189	2.695	3.710	62
13:00	MO	0	13.000	3.343	59.658	2.579	3.185	68
13:00	MO	-8	0.000	2.945	101.949	2.874	2.837	68
13:00	MO	-5	0.000	1.981	58.989	2.931	2.042	68
13:00	MO	0	0.000	3.463	45.790	2.465	3.312	68
13:00	MO	-5	0.000	3.777	72.62	3.65	3.921	68
13:00	MO	-3	0.000	3.857	39.591	2.873	3.666	68
13:00	MO	-1.5	0.000	4.707	0	2.822	4.514	68
13:00	MO	-3	0.000	2.448	36.835	2.339	1.993	68
13:00	MO	-1.5	0.000	1.784	16.898	2.206	1.629	68
13:13	MO	-8	0.000	3.567	16.622	2.658	3.443	68
13:13	MO	0	0.000	5.008	69.135	3.047	5.109	68
13:20	MO	0	0.000	5.222	44.122	3.051	5.032	68
13:26	MO	0	0.000	3.769	68.633	2.479	3.494	68
13:39	MO	0	14.000	4.091	36.202	2.669	3.684	68
13:39	MO	0	0.000	4.746	65.890	2.915	4.556	68
13:52	MO	0	0.000	4.703	58.734	2.976	4.425	68
14:00	MO	-8	0.000	4.070	31.007	3.381	4.173	68
14:00	MO	0	0.000	5.045	68.201	3.078	4.923	68
14:04	MO	0	0.000	5.171	59.784	3.191	4.926	68
14:12	MO	-8	0.000	2.565	22.117	2.423	2.418	68
14:12	MO	0	0.000	2.774	44.768	2.107	2.645	68
14:18	MO	0	0.000	5.254	17.271	3.063	4.923	68
14:26	MO	0	0.000	5.210	31.459	2.884	5.010	68
14:30	MO	0	0.000	5.222	16.068	2.773	4.981	68

14:37	MO	0	13.000	3.356	46.643	2.485	2.973	68
14:40	MO	0	0.000	3.302	46.243	2.771	3.010	68
14:45	MO	inj	0.000	6.156	13.39	2.403	4.401	68
14:45	MO	inj	0.000	6.164	12.661	2.667	4.465	68
14:49	MO	0	0.000	5.123	10.693	2.975	5.027	68
15:00	MO	0	0.000	5.149	14.041	2.699	4.844	68
15:00	MO	-8	0	4.577	24.165	3.637	4.631	68
15:06	MO	0	0.000	5.138	16.587	2.802	4.940	68
15:11	MO	0	0.000	5.151	33.537	2.913	4.880	68
15:14	MO	-8	0.000	4.460	24.416	3.338	4.365	68
15:16	MO	0	0.000	5.176	41.640	2.919	4.979	68
15:30	MO	0	0.000	5.076	27.907	3.415	4.955	68
15:30	MO	0	0.000	4.91	88.465	2.734	4.274	68
15:45	MO	0	15.000	5.314	16.002	2.963	4.761	68
15:53	MO	0	0.000	4.765	13.180	2.957	4.532	68
15:58	MO	0	10.000	5.040	30.403	3.014	4.890	68
16:00	MO	-8	0.000	3.132	19.124	2.807	2.991	68
16:05	MO	0	27.000	4.307	12.815	2.659	3.897	68
16:08	MO	0	0.000	5.012	43.239	3.070	4.851	68
16:11	MO	-8	0.000	4.473	25.658	3.04	4.326	68
16:17	MO	0	0.000	1.645	21.790	1.631	1.537	68
16:30	MO	0	19.000	5.276	36.432	3.167	4.705	68
16:30	MO	0	0.000	5.031	45.136	3.178	4.938	68
17:00	MO	0	0.000	4.302	32.802	3.033	4.287	68
17:00	MO	-8	0.000	4.366	26.527	3.325	4.359	68
17:00	MO	0	0.000	5.145	13.350	2.753	4.801	68
17:15	MO	0	14.000	5.219	18.522	2.802	4.592	68
17:15	MO	-8	0	4.437	23.965	3.271	4.244	68
17:15	MO	0	20.000	4.222	20.187	3.579	3.796	68
17:30	MO	0	0.000	5.966	12.207	2.802	4.496	68
17:30	MO	0	15.000	3.035	38.360	3.058	2.896	68
17:53	MO	0	0.000	4.979	33.848	2.981	4.681	68
17:53	MO	0	0.000	5.044	36.025	3.020	4.813	68
18:00	MO	0	10.000	4.892	25.812	2.982	4.573	68
18:00	MO	-8	0.000	4.402	26.718	3.045	4.263	68
18:00	MO	0	18.000	4.987	15.931	3.212	4.456	68
18:12	MO	0	0.000	4.942	37.095	2.923	4.866	68
18:12	MO	0	14.000	5.063	26.108	2.970	5.032	68
18:23	MO	inj	0.000	6.22	20.223	2.517	4.375	68
18:30	MO	0	14.000	5.071	25.308	2.953	4.957	68
18:30	MO	0	10.000	4.509	55.586	3.103	4.560	68
19:00	MO	0	0.000	3.154	27.563	2.290	2.733	68
19:00	MO	0	0.000	5.055	30.700	2.988	4.783	68

19:30	MO	0	12.000	5.042	13.624	2.747	4.875	68
19:30	MO	0	16.000	5.059	43.520	3.421	4.979	68
20:00	MO	0	0.000	4.912	17.548	2.501	4.326	68
20:00	MO	0	10.000	5.048	12.063	2.920	4.988	68
20:30	MO	0	0.000	4.840	44.039	2.986	4.198	68
20:30	MO	inj	0.000	5.622	19.766	2.929	4.787	68
20:30	MO	0	10.000	5.040	21.602	2.887	4.984	68
20:30	MO	inj	0.000	2.736	43.915	2.226	2.345	68
21:00	MO	0	0.000	5.771	14.500	2.405	4.442	68
21:00	MO	0	19.000	4.977	48.648	3.292	4.931	68
21:16	MO	-5	0.000	4.261	33.506	2.236	3.561	68
21:16	MO	-3	0.000	3.835	8.836	2.452	3.074	68
21:16	MO	-1.5	0.000	2.25	8.285	2.269	1.856	68
21:16	MO	-3	0.000	2.919	14.722	1.973	2.581	68
21:16	MO	-1.5	0.000	3.774	3.99	2.059	3.204	68
21:16	MO	0	17.000	3.428	15.706	2.665	3.306	68
21:16	MO	-8	0.000	4.15	90.492	2.287	3.478	68
21:16	MO	-5	0.000	4.842	29.028	2.07	3.825	68
21:16	MO	0	11.000	5.097	45.421	2.857	5.012	68
12:15	MC	0	13.000	5.941	37.456	2.783	5.850	61
12:28	MC	0	14.000	5.936	78.750	2.960	5.790	61
12:40	MC	0	16.000	5.821	21.252	2.476	4.347	61
12:53	MC	0	23.000	5.575	73.517	3.333	5.496	61
12:55	MC	inj	0.000	6.065	17.996	2.538	5.045	61
13:05	MC	0	14.000	6.004	21.268	2.713	5.347	61
13:20	MC	0	12.000	5.875	21.083	3.156	5.809	61
13:35	MC	0	16.000	5.849	38.895	2.772	5.715	61
13:50	MC	0	16.000	6.109	16.282	2.721	5.328	61
13:55	MC	inj	0.000	6.212	11.323	2.753	5.209	61
14:05	MC	0	11.000	5.633	99.846	3.078	5.580	61
14:20	MC	0	12.000	5.393	113.129	3.345	5.335	61
14:35	MC	0	0.000	5.829	41.695	3.042	5.412	61
14:39	MC	0	0.000	5.678	13.199	2.696	5.807	61
14:50	MC	0	11.000	3.240	72.683	2.675	3.296	61
15:05	MC	0	0.000	5.633	52.415	2.978	5.835	61
15:15	MC	inj	0.000	5.742	54.931	2.518	4.795	61
15:20	MC	0	0.000	5.549	70.340	3.056	5.811	61
15:35	MC	0	17.000	4.230	62.233	2.446	3.553	61
15:55	MC	0	16.000	3.936	77.065	2.469	4.094	61
16:05	MC	0	18.000	4.479	47.035	2.590	4.667	61
16:20	MC	0	14.000	2.836	52.863	3.786	2.377	61
16:30	MC	inj	20.000	5.543	110.431	2.842	5.071	61
16:35	MC	0	13.000	5.726	88.250	3.292	4.870	61

16:50	MC	0	13.000	3.154	47.808	2.149	2.633	61
17:05	MC	0	21.000	3.825	68.877	2.452	3.917	61
17:20	MC	0	13.000	5.677	76.795	3.091	4.846	61
17:35	MC	0	17.000	4.533	80.675	3.011	4.793	61
17:50	MC	0	20.000	5.207	81.913	3.155	5.559	61
18:00	MC	inj	13.000	2.432	43.750	3.941	1.943	61
18:05	MC	0	22.000	4.632	76.287	3.092	4.812	61
18:20	MC	0	18.000	5.413	88.386	2.989	5.578	61
18:35	MC	0	16.000	5.215	36.860	3.088	4.464	61
18:50	MC	0	14.000	5.758	28.109	3.023	4.991	61
18:55	MC	inj	0.000	3.810	60.321	2.373	3.182	61
19:05	MC	0	17.000	3.350	30.187	2.229	3.212	61
19:20	MC	0	0.000	4.615	29.141	2.223	4.105	61
19:35	MC	0	16.000	5.671	42.611	2.881	4.863	61
19:50	MC	0	24.000	3.788	60.511	4.694	3.268	61
20:05	MC	0	17.000	3.141	35.030	2.303	2.741	61
20:20	MC	0	15.000	5.105	12.867	2.659	4.388	61
20:35	MC	inj	20.000	5.511	43.031	2.813	5.015	61
20:35	MC	0	15.000	5.848	30.203	2.894	5.008	61
12:15	MO	-8	0.000	4.181	6.249	2.755	3.851	68
12:15	MO	0	10.000	5.049	24.160	3.011	5.015	68
12:15	MO	-8	0.000	4.445	6.637	2.876	4.057	68
12:15	MO	0	0.000	5.367	42.487	3.115	5.034	68
12:28	MO	0	14.000	5.038	28.632	3.062	5.070	68
12:28	MO	0	15.000	5.085	23.199	3.214	4.523	68
12:40	MO	-8	0.000	4.019	12.367	2.825	3.7	68
12:40	MO	0	13.000	5.199	13.781	2.893	4.605	68
12:40	MO	-8	0.000	4.352	16.146	2.735	3.779	68
12:40	MO	0	14.000	5.344	57.230	3.106	5.210	68
12:53	MO	0	13.000	1.955	22.694	n.a.	n.a.	68
12:53	MO	-8	0.000	4.815	50.338	3.211	3.96	68
12:53	MO	-5	0.000	3.695	26.825	2.997	3.12	68
12:53	MO	0	15.000	5.358	38.918	3.426	4.600	68
12:53	MO	-8	16.000	3.232	42.284	6.201	2.705	68
12:53	MO	-5	0.000	4.075	33.862	2.812	3.375	68
12:53	MO	-3	0.000	2.999	22.983	2.525	2.469	68
12:53	MO	-1.5	0.000	3.678	16.116	3.171	2.909	68
12:53	MO	-3	0.000	2.938	16.96	2.368	2.421	68
12:53	MO	-1.5	0.000	4.176	25.303	3.196	3.516	68
12:55	MO	inj	0.000	6.084	31.613	2.681	4.908	68
12:55	MO	inj	0.000	6.218	29.334	2.642	5.082	68
13:05	MO	0	13.000	5.230	15.709	3.357	5.003	68
13:05	MO	0	18.000	5.356	22.832	3.518	5.268	68

13:20	MO	0	17.000	5.040	25.884	3.730	4.981	68
13:20	MO	0	13.000	5.435	23.068	3.194	4.778	68
13:35	MO	-8	0.000	4.094	8.905	2.889	3.693	68
13:35	MO	0	19.000	4.977	56.322	3.751	4.885	68
13:35	MO	-8	0.000	4.379	15.803	3.369	4.048	68
13:35	MO	0	20.000	4.278	50.141	3.354	4.340	68
13:50	MO	-8	0.000	3.954	13.719	3.095	3.478	68
13:50	MO	0	16.000	5.051	47.981	4.300	4.981	68
13:50	MO	-8	0.000	4.427	11.132	3.422	3.987	68
13:50	MO	0	12.000	5.262	31.394	3.220	5.188	68
13:55	MO	inj	38.000	5.485	14.528	3.563	4.646	68
13:55	MO	inj	11.000	6.076	25.087	2.512	4.910	68
14:05	MO	0	14.000	5.303	12.757	3.329	4.513	68
14:05	MO	0	13.000	5.461	23.432	3.024	4.717	68
14:20	MO	0	15.000	5.205	16.002	3.489	4.491	68
14:20	MO	0	10.000	5.164	31.082	3.200	5.130	68
14:35	MO	-8	0	4.106	12.603	3.375	3.835	68
14:35	MO	0	13.000	4.941	19.129	3.724	4.935	68
14:35	MO	-8	0.000	3.607	9.448	2.618	3.205	68
14:35	MO	0	15.000	3.122	14.295	2.492	2.689	68
14:50	MO	-8	0.000	4.167	13.757	3.323	3.828	68
14:50	MO	0	12.000	2.747	26.117	3.649	2.770	68
14:50	MO	-8	0.000	3.726	12.875	2.809	3.37	68
14:50	MO	0	0.000	4.952	18.631	2.898	5.017	68
15:05	MO	0	12.000	4.806	19.999	3.557	4.976	68
15:05	MO	0	0.000	4.949	28.124	3.153	5.051	68
15:15	MO	inj	0.000	4.367	23.267	2.532	3.656	68
15:15	MO	inj	0.000	5.706	13.470	2.860	4.887	68
15:20	MO	0	0.000	1.006	10.571	1.745	1.000	68
15:20	MO	0	0.000	3.263	17.657	2.636	2.876	68
15:35	MO	-8	0.000	4.209	16.872	3.094	3.755	68
15:35	MO	0	15.000	1.117	9.928	2.245	1.224	68
15:35	MO	-8	0.000	2.83	16.818	3.164	2.494	68
15:35	MO	0	0.000	1.446	4.653	1.221	1.219	68
15:55	MO	-8	0.000	3.115	10.562	2.558	2.711	68
15:55	MO	0	15.000	5.128	9.275	3.344	4.500	68
15:55	MO	-8	0.000	4.308	12.450	2.612	3.798	68
15:55	MO	0	21.000	4.366	19.940	4.780	4.684	68
16:05	MO	0	16.000	4.795	14.143	3.499	4.935	68
16:05	MO	0	0.000	4.883	30.267	3.361	4.551	68
16:20	MO	0	0.000	4.727	14.557	3.040	4.264	68
16:20	MO	0	19.000	4.055	25.274	2.939	4.193	68
16:30	MO	inj	19.000	5.370	77.246	2.881	4.933	68

16:30	MO	inj	20.000	5.377	57.576	2.928	4.919	68
16:35	MO	-8	0.000	2.513	16.171	2.267	2.446	68
16:35	MO	0	0.000	4.812	23.519	3.538	4.515	68
16:35	MO	-8	0.000	2.886	15.846	2.539	2.701	68
16:35	MO	0	0.000	3.665	21.261	2.335	3.286	68
16:50	MO	-8	0	4.113	20.287	3.375	3.806	68
16:50	MO	0	16.000	3.716	19.531	3.046	3.183	68
16:50	MO	-8	0.000	3.977	21.850	3.238	3.877	68
16:50	MO	0	0.000	3.298	17.718	2.219	3.004	68
17:05	MO	0	29.000	3.447	22.949	2.966	3.493	68
17:05	MO	0	35.000	4.323	30.140	3.926	4.391	68
17:20	MO	0	13.000	3.211	18.382	2.560	2.739	68
17:20	MO	0	12.000	4.981	27.366	3.128	4.241	68
17:35	MO	-8	0.000	3.444	14.206	2.474	3.165	68
17:35	MO	0	16.000	3.099	22.126	2.501	3.219	68
17:35	MO	-8	0	4.099	21.329	3.634	3.829	68
17:50	MO	-8	0	4.205	18.372	3.895	3.877	68
17:50	MO	0	14.000	5.161	23.122	3.221	4.444	68
17:50	MO	-8	0.000	2.513	12.688	2.705	2.31	68
17:50	MO	0	0.000	4.976	18.558	3.143	4.436	68
18:00	MO	inj	23.000	2.288	58.565	3.510	2.082	68
18:00	MO	inj	0.000	5.435	96.022	3.423	4.950	68
18:05	MO	0	0.000	4.558	23.410	2.989	4.091	68
18:05	MO	0	18.000	4.465	22.230	2.754	4.494	68
18:20	MO	0	14.000	5.171	14.127	3.214	4.454	68
18:20	MO	0	29.000	4.850	26.948	3.581	4.907	68
18:35	MO	-8	0	4.148	21.924	8.688	3.757	68
18:35	MO	0	21.000	4.406	16.655	5.062	4.578	68
18:35	MO	-8	0.000	3.974	20.292	3.077	3.554	68
18:35	MO	0	14.000	4.439	15.926	2.988	3.411	68
18:50	MO	-8	0	4.366	14.489	4.036	4.018	68
18:50	MO	0	20.000	4.206	28.460	2.751	4.074	68
18:50	MO	-8	0.000	4.283	16.944	2.866	3.804	68
18:50	MO	0	23.000	2.137	11.283	2.219	2.017	68
18:55	MO	inj	0.000	3.350	45.213	2.071	2.748	68
18:55	MO	inj	0.000	5.686	79.594	2.947	4.880	68
19:05	MO	0	20.000	3.592	16.663	2.488	3.412	68
19:05	MO	0	0.000	2.580	11.194	2.059	2.038	68
19:20	MO	0	16.000	4.621	13.239	2.740	4.493	68
19:20	MO	0	0.000	5.053	7.998	2.659	4.520	68
19:35	MO	-8	0.000	2.889	21.185	2.361	2.473	68
19:35	MO	0	12.000	5.122	27.493	3.142	4.388	68
19:35	MO	-8	0	4.598	12.843	3.058	4.063	68

19:35	MO	0	18.000	4.361	21.231	2.862	4.709	68
19:50	MO	-8	0.000	4.575	6.983	2.639	4.015	68
19:50	MO	0	16.000	4.831	24.487	3.361	4.208	68
19:50	MO	-8	0	4.608	8.323	2.636	4.077	68
19:50	MO	0	19.000	5.137	8.401	3.057	4.481	68
20:05	MO	-8	0.000	4.223	18.895	3.212	3.702	68
20:05	MO	0	17.000	5.153	9.876	3.231	4.509	68
20:05	MO	-8	0	4.683	6.718	3.046	4.193	68
20:05	MO	0	17.000	4.431	21.166	3.403	3.906	68
20:20	MO	-8	0.000	4.444	16.409	2.835	4.009	68
20:20	MO	0	0.000	5.276	10.225	2.997	4.606	68
20:20	MO	-8	0	3.568	14.741	2.641	3.158	68
20:20	MO	0	17.000	4.906	10.600	2.776	4.793	68
20:35	MO	0	17.000	5.205	11.051	3.327	4.558	68
20:35	MO	inj	13.000	5.977	24.467	3.005	5.037	68
20:35	MO	-8	0.000	4.117	73.983	2.215	3.184	68
20:35	MO	-5	0.000	4.98	21.11	2.381	4.144	68
20:35	MO	-3	0.000	4.174	32.446	2.271	3.414	68
20:35	MO	0	17.000	5.203	12.973	2.903	4.483	68
20:35	MO	inj	0.000	5.880	35.690	2.755	4.885	68
20:35	MO	-8	0.000	3.747	22.951	2.473	2.699	68
20:35	MO	-5	0.000	5.36	41.539	2.339	3.856	68
20:35	MO	-3	0.000	4.901	17.434	n.a.	n.a.	68
20:35	MO	-1.5	0.000	5.232	5.179	2.582	3.905	68
20:35	MO	-1.5	0.000	4.8	35.908	2.552	3.339	68
10:05	MC-ac	0	16.000	6.341	43.780	3.127	5.431	60
12:00	MC-ac	inj	0.000	3.894	40.869	3.392	4.086	60
12:15	MC-ac	0	19.000	5.897	116.487	3.065	5.626	60
12:30	MC-ac	0	0.000	6.138	103.626	3.342	5.008	60
12:30	MC-ac	inj	0.000	3.801	72.743	2.503	2.984	60
12:45	MC-ac	0	21.000	5.560	102.208	3.229	5.612	60
13:15	MC-ac	0	18.000	6.001	100.372	3.202	5.191	60
13:30	MC-ac	0	19.000	5.008	97.821	3.209	5.159	60
13:30	MC-ac	inj	14.000	5.876	91.434	3.031	4.540	60
13:45	MC-ac	0	20.000	5.597	108.661	3.118	5.482	60
14:00	MC-ac	0	17.000	4.640	104.977	3.071	4.734	60
14:15	MC-ac	0	0.000	6.231	101.167	2.993	5.215	60
14:30	MC-ac	0	21.000	3.255	61.721	3.283	4.907	60
14:30	MC-ac	inj	12.000	5.897	92.722	3.470	4.847	60
14:45	MC-ac	0	0.000	5.847	99.289	3.155	5.169	60
15:00	MC-ac	0	17.000	4.615	95.296	3.106	4.054	60
15:15	MC-ac	0	19.000	5.816	98.042	3.085	5.005	60
15:30	MC-ac	0	0.000	5.716	97.331	2.991	5.080	60

15:30	MC-ac	inj	26.000	5.471	89.972	3.378	4.808	60
15:45	MC-ac	0	23.000	5.814	91.990	3.692	5.029	60
16:00	MC-ac	0	15.000	1.424	30.728	1.389	1.217	60
16:15	MC-ac	0	23.000	4.972	97.833	2.915	4.392	60
16:30	MC-ac	0	34.000	2.909	53.449	4.035	2.550	60
16:30	MC-ac	inj	10.000	5.469	89.118	3.424	4.786	60
16:45	MC-ac	0	19.000	5.677	88.762	3.293	4.899	60
17:00	MC-ac	0	19.000	5.340	89.417	3.286	4.412	60
17:15	MC-ac	0	19.000	1.928	19.510	1.539	1.633	60
17:30	MC-ac	0	13.000	5.781	75.042	3.229	4.286	60
17:30	MC-ac	inj	19.000	5.936	79.318	3.719	4.178	60
18:00	MC-ac	0	16.000	5.652	87.671	2.690	4.562	60
18:15	MC-ac	0	27.000	4.875	81.023	3.317	3.611	60
18:30	MC-ac	0	16.000	5.592	85.259	2.724	4.514	60
18:30	MC-ac	inj	0.000	5.865	73.601	3.187	4.280	60
18:45	MC-ac	0	21.000	5.630	82.341	2.765	4.569	60
19:00	MC-ac	0	25.000	5.441	93.031	2.785	4.495	60
19:15	MC-ac	0	22.000	5.497	91.256	3.265	5.034	60
19:30	MC-ac	0	17.000	5.516	83.609	3.173	4.861	60
19:30	MC-ac	inj	0.000	5.73	75.183	3.293	4.284	60
19:45	MC-ac	0	20.000	5.487	82.371	3.119	4.820	60
20:00	MC-ac	0	14.000	5.539	77.263	3.468	4.861	60
20:15	MC-ac	0	13.000	5.087	84.705	3.169	4.622	60
20:30	MC-ac	0	20.000	5.522	85.270	3.413	4.875	60
20:30	MC-ac	inj	15.000	6.02	70.05	3.713	4.187	60
20:45	MC-ac	0	29.000	3.268	59.335	3.633	2.938	60
21:00	MC-ac	0	23.000	5.489	75.448	3.749	4.860	60
10:05	MO-ac	0	0.000	6.37	44.163	7.686	4.784	66
12:00	MO-ac	inj	25.000	5.069	47.364	3.125	3.702	66
12:15	MO-ac	-8	0.000	5.164	12.931	3.691	4.452	66
12:15	MO-ac	0	0.000	6.181	90.325	8.215	5.106	66
12:30	MO-ac	-8	0.000	5.066	16.878	4.001	4.455	66
12:30	MO-ac	0	20.000	5.779	91.180	6.073	5.277	66
12:30	MO-ac	inj	23.000	4.709	82.157	2.932	4.252	66
12:45	MO-ac	0	19.000	5.880	92.058	5.584	4.928	66
13:15	MO-ac	-8	0	4.863	108.28	3.522	4.067	66
13:15	MO-ac	-5	0.000	4.739	61.041	3.478	4.084	66
13:15	MO-ac	-3	0.000	5.045	85.341	3.846	3.976	66
13:15	MO-ac	-1.5	0.000	5.519	85.006	2.577	4.212	66
13:15	MO-ac	0	21.000	5.635	84.126	6.248	5.174	66
13:30	MO-ac	-8	0.000	3.132	29.599	2.478	2.561	66
13:30	MO-ac	0	19.000	4.477	71.217	5.264	3.801	66
13:30	MO-ac	inj	28.000	5.401	93.903	3.213	4.674	66

13:45	MO-ac	0	19.000	5.689	81.619	5.961	4.834	66
14:00	MO-ac	0	16.000	5.395	80.171	5.465	5.085	66
14:15	MO-ac	-8	0.000	3.569	22.521	2.693	3.169	66
14:15	MO-ac	0	18.000	5.630	70.213	5.568	4.766	66
14:30	MO-ac	-8	0.000	4.402	30.021	2.842	3.851	66
14:30	MO-ac	0	0.000	5.937	67.761	5.374	4.684	66
14:30	MO-ac	inj	30.000	5.056	86.904	3.098	4.348	66
14:45	MO-ac	0	20.000	5.591	71.089	4.563	4.726	66
15:00	MO-ac	0	0.000	5.519	61.956	5.141	4.779	66
15:15	MO-ac	-8	0	4.337	24.084	3.372	3.911	66
15:15	MO-ac	0	17.000	5.532	61.626	4.048	4.674	66
15:30	MO-ac	-8	0.000	4.439	27.035	3.008	4.019	66
15:30	MO-ac	0	16.000	5.465	62.961	4.476	4.682	66
15:30	MO-ac	inj	10.000	5.192	89.437	2.993	4.600	66
15:45	MO-ac	0	28.000	5.476	57.711	4.629	4.677	66
16:00	MO-ac	0	20.000	5.413	56.196	4.016	4.650	66
16:15	MO-ac	-8	0	4.17	27.037	4.452	3.688	66
16:15	MO-ac	0	20.000	5.332	54.232	3.857	4.637	66
16:30	MO-ac	-8	0	2.916	17.741	n.a.	n.a.	66
16:30	MO-ac	0	19.000	4.967	48.332	3.782	4.263	66
16:30	MO-ac	inj	15.000	5.466	89.582	3.187	4.822	66
16:45	MO-ac	0	32.000	5.075	50.328	3.768	4.342	66
17:00	MO-ac	0	23.000	4.559	50.172	2.935	3.750	66
17:15	MO-ac	-8	0	2.446	5.249	2.252	2.105	66
17:15	MO-ac	0	24.000	3.711	76.997	2.276	2.946	66
17:30	MO-ac	-8	0.000	5.282	29.575	3.825	4.043	66
17:30	MO-ac	0	27.000	4.237	74.680	2.836	3.582	66
17:30	MO-ac	inj	0.000	5.871	11.448	2.399	4.372	66
18:00	MO-ac	0	23.000	5.277	35.464	3.039	4.234	66
18:15	MO-ac	-8	0	4.638	23.285	2.316	4.077	66
18:15	MO-ac	0	18.000	5.226	38.199	2.791	4.268	66
18:30	MO-ac	-8	0	4.737	24.169	2.762	4.308	66
18:30	MO-ac	0	23.000	5.066	37.272	2.795	4.328	66
18:30	MO-ac	inj	0.000	5.818	76.469	2.728	3.836	66
18:45	MO-ac	0	20.000	5.207	37.968	2.661	4.145	66
19:00	MO-ac	0	24.000	5.084	41.875	2.821	4.264	66
19:15	MO-ac	-8	0.000	4.859	26.594	2.281	4.146	66
19:15	MO-ac	0	24.000	5.234	31.131	3.395	4.651	66
19:30	MO-ac	-8	0.000	4.129	28.117	2.424	4.167	66
19:30	MO-ac	0	20.000	4.858	38.658	3.009	4.295	66
19:30	MO-ac	inj	0.000	6.183	83.119	3.016	4.423	66
19:45	MO-ac	0	20.000	5.175	43.260	3.010	4.542	66
20:00	MO-ac	0	0.000	4.655	37.776	2.961	4.042	66

20:15	MO-ac	-8	0	4.294	28.119	2.562	4.192	66
20:15	MO-ac	0	28.000	4.403	34.394	3.138	3.572	66
20:30	MO-ac	0	0.000	5.363	43.044	3.071	4.636	66
20:30	MO-ac	inj	0.000	2.646	42.364	1.770	2.065	66
20:30	MO-ac	-8	0.000	5.126	98.755	2.222	4.222	66
20:30	MO-ac	-5	0.000	5.124	44.263	2.422	4.063	66
20:30	MO-ac	-3	0.000	5.41	48.12	2.303	3.681	66
20:30	MO-ac	-1.5	0.000	3.968	45.167	2.629	3.146	66
20:45	MO-ac	0	0.000	4.016	38.679	3.106	3.469	66
21:00	MO-ac	0	0.000	5.983	44.132	n.a.	n.a.	66
back	MO-ac	-8	0	1.834	16.351	n.a.	n.a.	66
10:05	MO-c	0	0.000	3.735	49.955	4.215	2.814	66
12:00	MO-c	inj	0.000	4.177	16.692	1.767	1.600	66
12:15	MO-c	-8	0.000	4.883	16.578	3.072	4.456	66
12:15	MO-c	0	0.000	5.983	32.102	3.994	5.133	66
12:30	MO-c	-8	0	4.869	27.877	3.623	4.418	66
12:30	MO-c	0	18.000	5.794	22.408	3.596	5.000	66
12:30	MO-c	inj	10.000	5.900	44.459	2.813	4.899	66
12:45	MO-c	0	14.000	5.738	27.411	3.370	4.957	66
13:15	MO-c	-3	0.000	5.18	37.292	2.746	4.166	66
13:15	MO-c	-1.5	0.000	5.241	15.023	4.116	4.347	66
13:15	MO-c	-8	0	5.446	95.477	2.829	3.478	66
13:15	MO-c	-5	0.000	5.12	63.81	2.612	4.075	66
13:15	MO-c	0	0.000	5.797	26.740	3.649	4.959	66
13:30	MO-c	-8	0.000	4.07	34.900	2.937	4.003	66
13:30	MO-c	0	0.000	4.185	40.536	2.794	3.438	66
13:30	MO-c	inj	0.000	5.005	82.333	3.632	4.080	66
13:45	MO-c	0	15.000	5.480	19.085	3.313	4.846	66
14:00	MO-c	0	17.000	5.468	15.607	3.027	4.767	66
14:15	MO-c	-8	0.000	3.27	25.270	3.164	3.032	66
14:15	MO-c	0	17.000	4.991	32.632	2.701	4.503	66
14:30	MO-c	-8	0	4.634	6.659	3.31	4.173	66
14:30	MO-c	0	0.000	5.595	43.307	3.314	4.737	66
14:30	MO-c	inj	0.000	4.959	52.504	2.582	4.116	66
14:45	MO-c	0	16.000	3.532	23.955	4.031	4.311	66
15:00	MO-c	0	15.000	5.290	24.956	2.959	4.633	66
15:15	MO-c	-8	0.000	3.631	24.715	2.65	3.328	66
15:15	MO-c	0	0.000	4.617	42.958	2.788	4.155	66
15:30	MO-c	-8	0.000	4.601	15.511	2.919	4.261	66
15:30	MO-c	0	17.000	5.213	13.210	2.849	4.553	66
15:30	MO-c	inj	0.000	5.358	78.430	2.880	4.811	66
15:45	MO-c	0	17.000	4.854	26.994	2.589	4.388	66
16:00	MO-c	0	20.000	4.360	29.860	2.707	3.866	66

16:15	MO-c	-8	0	4.016	21.949	4.005	3.731	66
16:15	MO-c	0	19.000	2.815	25.488	3.754	2.334	66
16:30	MO-c	-8	0.000	3.359	20.415	2.928	3.11	66
16:30	MO-c	0	18.000	4.482	31.182	2.820	3.918	66
16:30	MO-c	inj	18.000	5.355	15.172	2.618	4.816	66
16:45	MO-c	0	22.000	3.399	27.087	2.433	2.869	66
17:00	MO-c	0	21.000	4.846	15.925	2.403	4.095	66
17:15	MO-c	-8	0.000	3.309	24.012	2.192	2.951	66
17:15	MO-c	0	n.a.	n.a.	n.a.	3	3.787	66
17:30	MO-c	-8	0.000	3.525	24.652	2.351	3.058	66
17:30	MO-c	0	n.a.	n.a.	n.a.	2.482	3.945	66
17:45	MO-c	0	0.000	4.585	4.73	3.028	3.510	66
18:00	MO-c	0	23.000	4.808	23.755	2.370	4.075	66
18:15	MO-c	-8	0.000	1.613	11.476	1.642	1.465	66
18:15	MO-c	0	18.000	5.119	9.616	2.334	4.031	66
18:30	MO-c	-8	0.000	2.961	7.724	1.632	2.645	66
18:30	MO-c	0	18.000	5.026	15.646	2.514	4.156	66
18:30	MO-c	inj	0.000	5.754	7.986	2.298	4.261	66
18:45	MO-c	0	23.000	5.025	9.342	2.996	4.165	66
19:00	MO-c	0	19.000	4.683	11.977	2.339	3.904	66
19:15	MO-c	-8	0.000	4.657	5.348	2.119	4.056	66
19:15	MO-c	0	24.000	4.943	11.665	2.767	4.483	66
19:30	MO-c	-8	0.000	4.66	14.310	2.312	4.027	66
19:30	MO-c	0	19.000	4.858	10.286	3.048	4.998	66
19:30	MO-c	inj	0.000	6.217	12.842	2.211	3.823	66
19:45	MO-c	0	20.000	5.008	12.042	2.720	4.345	66
20:00	MO-c	0	19.000	4.967	17.364	2.858	4.526	66
20:15	MO-c	-8	0.000	4.159	12.790	2.205	4.043	66
20:15	MO-c	0	20.000	5.000	14.907	2.871	4.536	66
20:30	MO-c	-8	0.000	2.295	66.721	1.354	1.595	66
20:30	MO-c	-5	0.000	4.958	40.57	2.473	4.036	66
20:30	MO-c	0	0.000	5.192	11.154	2.799	4.595	66
20:30	MO-c	inj	0.000	6.074	11.918	2.318	4.446	66
20:30	MO-c	-3	0.000	5.037	32.913	2.163	4.192	66
20:30	MO-c	-1.5	0.000	5.075	19.488	2.278	4.122	66
20:45	MO-c	0	22.000	3.266	8.337	2.789	2.960	66
21:00	MO-c	0	0.000	5.786	20.026	2.356	4.050	66
back	MO-c	-8	0	5.031	35.641	3.828	4.713	66

A.4 Method for Fluorescence and PARAFAC Analysis

Water samples for fluorescence analysis were frozen with dry ice immediately following sampling. Samples were kept frozen until fluorescence analysis. Samples were thawed completely before taking absorbance scans from 240-550 nm. Water samples were diluted with Milli-Q water to an absorbance below 0.20 in order to avoid inner filter effects. EEMs were created by measuring fluorescence intensity across the excitation wavelengths of 240-450 nm (every 5 nm) and emission wavelengths from 350-550 nm (every 2 nm). Excitation and emission slit widths were 5 nm. EEMs were corrected within MATLAB for instrument bias, absorption, and Raman normalized using an EEM of Milli-Q water.

The corrected EEMs were analyzed using the PARAFAC model in order to determine DOM characterization. DOM characterization has a strong influence on the role DOM can play in the environment, for example, DOM characteristics influence how easily the DON and DOC contained within the DOM can be accessed and metabolized [*Fellman et al.*, 2009]. Fluorescence can detect the optically active fractions of DOM. Changes in DOM composition can be traced with fluorescence because biochemical characteristics of DOM can be related to its optical properties [*Fellman et al.*, 2009; *Stedmon et al.*, 2003]. The PARAFAC model tries to create a best fit for the sample EEMs to EEMs with known optical properties. The PARAFAC model can then provide information on the source, redox state, and biological reactivity of a sample's DOM. Table A.4.1 provides the PARAFAC output for samples from this experiment.

Table A.4.1: PARAFAC model output for MO-ac, MO-c, and MC-ac. n.a. denotes not available.

Depth	Mesocosm	Time	%C1	%C2 (Q2)	%C3	%C4 (HQ)	%C5 (SQ1)	%C6	%C7 (SQ2)	%C8 (Tryptophan)	%C9 (SQ3)	%C10	%C11 (Q1)	%C12 (Q3)	%C13 (Tyrosine)	Absorbance at 254nm	DOC (mg/L)	SUVA (L/mg C/m)	FI	Protien	RI	HQ/Q2
0	MO-ac	13:15	0%	18%	0%	26%	21%	35%	0%	0%	0%	0%	0%	0%	0%	0.0515	6.248	0.82	1.56	0%	0.722	1.5
1.5	MO-ac	13:15	0%	9%	0%	19%	23%	48%	0%	0%	0%	0%	0%	0%	0%	0.0614	2.577	2.38	1.57	0%	0.823	2.1
3	MO-ac	13:15	0%	9%	0%	19%	20%	51%	0%	0%	0%	0%	0%	0%	0%	0.0560	3.846	1.46	1.57	0%	0.810	2.1
5	MO-ac	13:15	0%	11%	0%	28%	21%	40%	0%	0%	0%	0%	0%	0%	0%	0.0498	3.478	1.43	1.57	0%	0.808	2.4
8	MO-ac	13:15	0%	16%	0%	10%	23%	40%	0%	0%	0%	11%	0%	0%	0%	0.0422	3.522	1.20	1.56	0%	0.681	0.7
0	MO-ac	14:30	0%	15%	0%	42%	15%	19%	0%	9%	0%	0%	0%	2%	0%	0.0532	5.374	0.99	1.55	9%	0.779	2.9
1.5	MO-ac	14:30	0%	26%	0%	35%	6%	13%	0%	6%	0%	0%	0%	12%	0%	0.0531	3.548	1.50	1.54	6%	0.520	1.4
3	MO-ac	14:30	0%	24%	0%	35%	11%	14%	0%	7%	0%	0%	0%	8%	0%	0.0521	3.584	1.45	1.57	7%	0.586	1.4
5	MO-ac	14:30	0%	10%	0%	16%	1%	0%	0%	44%	0%	0%	0%	28%	0%	0.0541	3.356	1.61	1.58	44%	0.314	1.6
0	MO-ac	15:30	0%	21%	0%	36%	11%	20%	0%	8%	0%	0%	0%	5%	0%	0.0515	4.476	1.15	1.57	8%	0.642	1.7
1.5	MO-ac	15:30	0%	13%	0%	35%	22%	23%	0%	8%	0%	0%	0%	0%	0%	0.0482	2.693	1.79	1.50	8%	0.814	2.7
3	MO-ac	15:30	0%	23%	0%	37%	5%	17%	0%	6%	0%	0%	0%	12%	0%	0.0514	2.905	1.77	1.55	6%	0.540	1.6
5	MO-ac	15:30	0%	23%	0%	40%	4%	15%	0%	6%	0%	0%	0%	12%	0%	0.0509	2.663	1.91	1.55	6%	0.555	1.7
0	MO-ac	18:30	0%	19%	0%	30%	13%	23%	0%	10%	0%	0%	0%	6%	0%	0.0615	2.795	2.20	1.58	10%	0.633	1.5
1.5	MO-ac	18:30	0%	22%	0%	30%	14%	17%	0%	9%	0%	0%	0%	8%	0%	0.0525	2.696	1.95	1.56	9%	0.591	1.3
3	MO-ac	18:30	0%	21%	0%	32%	12%	16%	0%	9%	0%	0%	0%	9%	0%	0.0570	2.615	2.18	1.56	9%	0.593	1.5
5	MO-ac	18:30	0%	21%	0%	33%	9%	17%	0%	8%	0%	0%	0%	11%	0%	0.0604	2.504	2.41	1.54	8%	0.571	1.5
8	MO-ac	18:30	0%	22%	0%	33%	11%	19%	0%	7%	0%	0%	0%	9%	0%	0.0542	2.762	1.96	1.55	7%	0.588	1.5
0	MO-ac	19:30	0%	22%	0%	30%	16%	32%	0%	0%	0%	0%	0%	0%	0%	0.0576	3.009	1.91	1.56	0%	0.681	1.4
1.5	MO-ac	19:30	0%	22%	0%	35%	16%	21%	0%	4%	0%	0%	0%	2%	0%	0.0596	2.943	2.03	1.58	4%	0.681	1.6
3	MO-ac	19:30	0%	25%	0%	35%	8%	15%	0%	6%	0%	0%	0%	11%	0%	0.0613	2.634	2.33	1.52	6%	0.535	1.4
5	MO-ac	19:30	1%	27%	0%	32%	9%	13%	0%	8%	0%	0%	0%	10%	0%	0.0554	2.702	2.05	1.53	8%	0.524	1.2
8	MO-ac	19:30	0%	20%	0%	29%	25%	19%	0%	7%	0%	0%	0%	0%	0%	0.0602	2.424	2.48	1.55	7%	0.732	1.5

0	MO-ac	20:30	0%	17%	0%	38%	8%	17%	0%	8%	0%	0%	0%	13%	0%	0.0571	3.071	1.86	1.58	8%	0.609	2.3
1.5	MO-ac	20:30	0%	14%	0%	40%	13%	21%	0%	7%	0%	0%	0%	6%	0%	0.0623	2.629	2.37	1.56	7%	0.729	2.9
3	MO-ac	20:30	0%	14%	0%	36%	12%	32%	0%	4%	0%	0%	0%	2%	0%	0.0604	2.303	2.62	1.58	4%	0.744	2.5
5	MO-ac	20:30	0%	11%	0%	37%	20%	25%	0%	7%	0%	0%	0%	0%	0%	0.0573	2.422	2.37	1.59	7%	0.833	3.2
8	MO-ac	20:30	0%	14%	0%	31%	16%	38%	0%	2%	0%	0%	0%	0%	0%	0.0566	2.222	2.55	1.55	2%	0.771	2.2
1.5	MO-c	13:15	0%	3%	0%	18%	27%	51%	0%	0%	0%	0%	0%	0%	0%	0.0654	4.116	1.59	1.60	0%	0.937	5.9
3	MO-c	13:15	0%	15%	0%	27%	21%	37%	0%	0%	0%	0%	0%	0%	0%	0.0631	2.746	2.30	1.60	0%	0.766	1.9
0	MO-c	13:15	0%	7%	0%	6%	22%	65%	0%	0%	0%	0%	0%	0%	0%	0.0781	3.649	2.14	1.56	0%	0.802	0.8
5	MO-c	13:15	0%	14%	0%	15%	19%	51%	0%	0%	0%	0%	0%	0%	0%	0.0629	2.612	2.41	1.58	0%	0.704	1.1
8	MO-c	13:15	0%	17%	0%	6%	10%	64%	0%	0%	0%	0%	3%	0%	0%	0.0620	2.829	2.19	1.55	0%	0.443	0.4
0	MO-c	14:30	0%	19%	0%	33%	18%	30%	0%	0%	0%	0%	0%	0%	0%	0.0483	3.314	1.46	1.57	0%	0.729	1.7
8	MO-c	14:30	0%	20%	0%	14%	27%	39%	0%	0%	0%	0%	0%	0%	0%	0.0358	3.31	1.08	1.58	0%	0.670	0.7
1.5	MO-c	14:30	0%	11%	0%	0%	14%	0%	0%	0%	0%	75%	0%	0%	0%	0.0472	n.a.	n.a.	1.50	0%	0.563	0.0
3	MO-c	14:30	0%	22%	0%	34%	18%	18%	0%	7%	0%	0%	0%	2%	0%	0.0681	3.568	1.91	1.54	7%	0.687	1.6
5	MO-c	14:30	2%	26%	0%	9%	21%	21%	0%	0%	0%	21%	0%	0%	0%	0.0522	1.77	2.95	1.52	0%	0.532	0.3
1.5	MO-c	15:30	0%	0%	0%	19%	35%	46%	0%	0%	0%	0%	0%	0%	0%	0.0500	n.a.	n.a.	1.54	0%	1.000	n.a.
3	MO-c	15:30	0%	22%	0%	0%	14%	0%	2%	5%	0%	57%	0%	0%	0%	0.0497	3.604	1.38	1.54	5%	0.413	0.0
0	MO-c	15:30	0%	5%	0%	19%	25%	52%	0%	0%	0%	0%	0%	0%	0%	0.0544	2.849	1.91	1.60	0%	0.901	3.9
5	MO-c	15:30	0%	14%	0%	34%	17%	25%	0%	8%	0%	0%	0%	1%	0%	0.0496	1.817	2.73	1.46	8%	0.763	2.4
8	MO-c	15:30	0%	4%	0%	18%	23%	54%	0%	0%	0%	0%	0%	0%	0%	0.0612	2.919	2.10	1.55	0%	0.917	4.9
1.5	MO-c	18:30	0%	23%	0%	36%	7%	18%	0%	5%	0%	0%	0%	10%	0%	0.0516	2.313	2.23	1.57	5%	0.567	1.6
3	MO-c	18:30	0%	25%	0%	34%	6%	13%	0%	8%	0%	2%	0%	13%	0%	0.0527	2.342	2.25	1.60	8%	0.516	1.4
5	MO-c	18:30	0%	11%	0%	29%	28%	32%	0%	1%	0%	0%	0%	0%	0%	0.0657	2.068	3.18	1.57	1%	0.843	2.7
0	MO-c	18:30	1%	3%	0%	8%	22%	66%	0%	0%	0%	0%	0%	0%	0%	0.0806	2.514	3.21	1.52	0%	0.917	3.1
8	MO-c	18:30	0%	8%	0%	19%	18%	55%	0%	0%	0%	0%	0%	0%	0%	0.0538	1.632	3.30	1.57	0%	0.823	2.4
0	MO-c	19:30	0%	9%	0%	23%	28%	38%	0%	2%	0%	0%	0%	0%	0%	0.0747	3.048	2.45	1.62	2%	0.855	2.6
1.5	MO-c	19:30	0%	22%	0%	33%	18%	23%	0%	3%	0%	0%	0%	0%	0%	0.0573	2.558	2.24	1.60	3%	0.702	1.5
3	MO-c	19:30	0%	21%	0%	33%	21%	22%	0%	4%	0%	0%	0%	0%	0%	0.0596	2.594	2.30	1.57	4%	0.723	1.6
5	MO-c	19:30	0%	19%	0%	35%	17%	24%	0%	4%	0%	0%	0%	1%	0%	0.0570	2.344	2.43	1.58	4%	0.716	1.8
8	MO-c	19:30	0%	13%	0%	31%	24%	32%	0%	0%	0%	0%	0%	0%	0%	0.0637	2.312	2.76	1.60	0%	0.801	2.3

0	MO-c	20:30	0%	17%	0%	11%	17%	50%	0%	0%	0%	0%	6%	0%	0%	0.0618	2.799	2.21	1.60	0%	0.548	0.6
8	MO-c	20:30	0%	2%	0%	7%	22%	67%	0%	0%	0%	0%	2%	0%	0%	0.0657	1.354	4.85	1.48	0%	0.885	3.8
1.5	MO-c	20:30	0%	8%	0%	37%	23%	28%	0%	4%	0%	0%	0%	0%	0%	0.0573	2.278	2.52	1.57	4%	0.882	4.6
3	MO-c	20:30	0%	3%	0%	30%	26%	41%	0%	0%	0%	0%	0%	0%	0%	0.0563	2.163	2.60	1.56	0%	0.949	10.1
5	MO-c	20:30	0%	11%	0%	19%	15%	53%	0%	0%	0%	0%	2%	0%	0%	0.0641	2.473	2.59	1.58	0%	0.730	1.8
0	MC-ac	13:15	0%	24%	0%	38%	10%	22%	0%	0%	0%	0%	0%	7%	0%	0.0442	3.202	1.38	1.55	0%	0.610	1.6
0	MC-ac	14:30	0%	19%	0%	33%	10%	19%	0%	9%	0%	0%	0%	9%	0%	0.0557	3.283	1.70	1.55	9%	0.608	1.8
0	MC-ac	15:30	0%	18%	0%	36%	16%	22%	0%	7%	0%	0%	0%	2%	0%	0.0565	2.991	1.89	1.54	7%	0.726	2.0
0	MC-ac	18:30	0%	20%	0%	33%	14%	28%	0%	4%	0%	0%	0%	1%	0%	0.0686	2.724	2.52	1.55	4%	0.688	1.7
0	MC-ac	19:30	0%	19%	0%	35%	19%	24%	0%	3%	0%	0%	0%	0%	0%	0.0585	3.173	1.84	1.56	3%	0.744	1.9
0	MC-ac	20:30	3%	0%	0%	11%	41%	6%	20 %	5%	0%	11%	0%	4%	0%	0.0543	3.413	1.59	1.58	5%	0.952	n.a.

Appendix B: Statistical Analysis

B.1 Cumulative mass load regression analysis

NO_x, NH_4^+, PO_4^{3-}, and DOC data for this experiment were taken at various times throughout the day. This creates some dependence between points. In order to remove this serial correlation between data points, cumulative mass load regressions were used. Since the cumulative mass load regression starts at zero (i.e. the cumulative mass load at the start of the experiment was zero), a regression forcing the intercepts through zero was used to test whether the slopes of the inlet and outlet cumulative mass loads were different (alpha = 0.05). The null and alternative hypotheses were as follows:

H_{O1}: $\mu_{inlet} = \mu_{outlet}$: The slope of the regression for the inlet is equal to the slope of the regression for the outlet.

H_{A1}: $\mu_{inlet} \neq \mu_{outlet}$: The slope of the regression for the inlet is not equal to the slope of the regression for the outlet.

The p-value for the variable time*dummy is the probability the slopes are equal. The coefficient for the time*dummy variable is the nutrient or carbon removal occurring within the mesocosm with the units of load/time. The following example (DOC data for MO) outlines the commands used in R to implement this analysis and develop the graphs.

```
> x<- read.csv("DOC.csv")
> attach(x)
> names(x)
"time"     "doc.load" "site"     "day"      "mesocosm"
> dummy <- ifelse(site=="inlet",0,1)
> lm.doc <- lm(doc.load~time+I(time*dummy)+0)
> summary(lm.doc)

Call:
lm(formula = doc.load ~ time + I(time * dummy) + 0)
```

Residuals:

Min	1Q	Median	3Q	Max
-10.3357	-2.6075	-0.3968	3.1520	12.3380

Coefficients:

	Estimate	Std. Error	t value	Pr(>|t|)
time	0.208122	0.001510	137.820	< 2e-16 ***
I(time * dummy)	0.011577	0.002501	4.629	8.27e-06 ***

Signif. codes: 0 '***' 0.001 '**' 0.01 '*' 0.05 '.' 0.1 ' ' 1

Residual standard error: 4.181 on 141 degrees of freedom
Multiple R-squared: 0.9955, Adjusted R-squared: 0.9954
F-statistic: 1.557e+04 on 2 and 141 DF, p-value: < 2.2e-16

```
> doc.in.time <- time[site=="inlet"]
> doc.in.load <- doc.load[site=="inlet"]
> doc.out.time <- time[site!="inlet"]
> doc.out.load <- doc.load[site!="inlet"]
> plot(doc.in.time, doc.in.load, pch=18, col="blue", xlim=c(0,650), ylim=c(0,150), xlab="Time
(minutes)", ylab="DOC, cumulative load (mg)")
> abline(lm(doc.in.load~doc.in.time+0), lty=1, lwd=2, col="blue")
> points(doc.out.time, doc.out.load, pch=19, col="red")
> abline(lm(doc.out.load~doc.out.time+0), lty=2, lwd=2, col="red")
> legend("topleft", legend=c("inlet", "outlet"), lty=c(1,2), lwd=c(2,2), pch=c(18.19),
col=c("blue", "red"))
> grid()
```

B.2 ANOVA/ANCOVA and Tukey HSD analysis of PARAFAC model results

In order to compare PARAFAC model results, surface water results were compared among MO-ac, MO-c, and MC-ac while subsurface results were compared between MO-ac and MO-c. Surface and subsurface results were analyzed to determine whether DOM characterization changed with time, depth, treatment (i.e. MO-c, MO-ac, or MC-ac) and/or higher interactions. Significant interactions were determined using an ANCOVA in SAS with time and depth as categorical data. Since the higher order interactions do not have replicates, p-values could not be obtained. The model was then chosen by dropping the smallest Type III mean squared and re-running the model. An ANOVA in R was also used to determine whether or not there were significant differences with time, depth, treatment, and/or their interactions. R returned a p-value

for the higher interactions so these results were used to verify the model in SAS. Once a model was determined to be significant, a Tukey HSD was applied to determine which categories of time, depth, treatment, and/or their interactions were different. The R code for this analysis along with the results from R and SAS are given below.

- ***Protein: Surface water ANOVA in R***

```
> x <- read.csv("Proteins.csv")
> attach(x)
> summary(aov(protein~time*mesocosm))
```

	Df	Sum Sq	Mean Sq	F value	Pr(>F)
time	1	0.0002976	0.0002976	0.2326	0.63828
mesocosm	2	0.0100778	0.0050389	3.9381	0.04843 *
time:mesocosm	2	0.0000981	0.0000490	0.0383	0.96251
Residuals	12	0.0153543	0.0012795		

Signif. codes: 0 ‘***’ 0.001 ‘**’ 0.01 ‘*’ 0.05 ‘.’ 0.1 ‘ ’ 1

- ***Protein: Surface water ANCOVA in SAS with Tukey’s HSD***

Tukey's Studentized Range (HSD) Test for protein

Alpha	0.05
Error Degrees of Freedom	10
Error Mean Square	0.000792
Critical Value of Studentized Range	3.87678
Minimum Significant Difference	0.0445

Means with the same letter are not significantly different.

Tukey Grouping	Mean	N	mesocosm
A	0.05833	6	M1
B A	0.04667	6	MC
B	0.00333	6	M2

- ***Protein: Subsurface water ANOVA in R***

```
> x <- read.csv("Protein.csv")
> attach(x)
> y <- aov(protein~time*depth*mesocosm)
> summary(y)
```

	Df	Sum Sq	Mean Sq	F value	Pr(>F)
time	1	0.000720	0.000720	0.1866	0.667574
depth	1	0.000503	0.000503	0.1302	0.719673
mesocosm	1	0.032202	0.032202	8.3425	0.005633 **
time:depth	1	0.000341	0.000341	0.0884	0.767396
time:mesocosm	1	0.000007	0.000007	0.0018	0.966195
depth:mesocosm	1	0.000000	0.000000	0.0001	0.991138
time:depth:mesocosm	1	0.000008	0.000008	0.0020	0.964554
Residuals	52	0.200717	0.003860		

Signif. codes: 0 '***' 0.001 '**' 0.01 '*' 0.05 '.' 0.1 ' ' 1

- ***Protein: Subsurface water ANCOVA in SAS with Tukey's HSD***

Dependent Variable: protein

Source	DF	Sum of Squares	Mean Square	F Value	Pr > F
Model	1	0.03220167	0.03220167	9.23	0.0036
Error	58	0.20229667	0.00348787		
Corrected Total	59	0.23449833			

R-Square	Coeff Var	Root MSE	protein Mean
0.137322	147.0329	0.059058	0.040167

Source	DF	Type I SS	Mean Square	F Value	Pr > F
mesocosm	1	0.03220167	0.03220167	9.23	0.0036

Source	DF	Type III SS	Mean Square	F Value	Pr > F
mesocosm	1	0.03220167	0.03220167	9.23	0.0036

Tukey's Studentized Range (HSD) Test for protein

Alpha	0.05
Error Degrees of Freedom	58
Error Mean Square	0.003488
Critical Value of Studentized Range	2.83086
Minimum Significant Difference	0.0305

Means with the same letter are not significantly different.

Tukey Grouping	Mean	N	mesocosm
A	0.06333	30	M1
B	0.01700	30	M2

- ***RI: Surface water ANOVA in R***

```
> x <- read.csv("RIs.csv")
> attach(x)
> y <- aov(ri~time*depth*mesocosm)
> summary(y)
```

	Df	Sum Sq	Mean Sq	F value	Pr(>F)
time	1	0.000517	0.000517	0.0555	0.81766
mesocosm	2	0.039853	0.019926	2.1394	0.16046
time:mesocosm	2	0.083223	0.041612	4.4676	0.03547 *
Residuals	12	0.111770	0.009314		

Signif. codes: 0 '***' 0.001 '**' 0.01 '*' 0.05 '.' 0.1 ' ' 1

- ***RI: Surface water ANCOVA in SAS with Tukey's HSD***

Dependent Variable: ri

Source	DF	Sum of Squares	Mean Square	F Value	Pr > F
Model	17	0.23536351	0.01384491	.	.
Error	0	0.00000000	.		
Corrected Total	17	0.23536351			

R-Square	Coeff Var	Root MSE	ri Mean
1.000000	.	.	0.730151

Source	DF	Type I SS	Mean Square	F Value	Pr > F
time*mesocosm	17	0.23536351	0.01384491	.	.

Source	DF	Type III SS	Mean Square	F Value	Pr > F
time*mesocosm	17	0.23536351	0.01384491	.	.

Level of time	Level of mesocosm	N	ri Mean	ri Std Dev
1	M1	1	0.72175896	.
1	M2	1	0.80181675	.
1	MC	1	0.60956779	.
2	M1	1	0.77940420	.
2	M2	1	0.72934525	.
2	MC	1	0.60781248	.
3	M1	1	0.64217931	.
3	M2	1	0.90079468	.
3	MC	1	0.72577907	.
4	M1	1	0.63263050	.
4	M2	1	0.91667510	.
4	MC	1	0.68784084	.
5	M1	1	0.68105964	.
5	M2	1	0.85450040	.
5	MC	1	0.74393427	.
6	M1	1	0.60851294	.
6	M2	1	0.54751364	.
6	MC	1	0.95159982	.

Tukey's HSD cannot tell what is significantly different with time*mesocosm since there are no replicates.

- ***RI: Subsurface water ANOVA in R***

```
> x <- read.csv("RI.csv")
> attach(x)
> y <- aov(ri~time*depth*mesocosm)
> summary(y)
```

	Df	Sum Sq	Mean Sq	F value	Pr(>F)
time	1	0.01121	0.011212	0.5851	0.44778
depth	1	0.00212	0.002124	0.1108	0.74056
mesocosm	1	0.09546	0.095464	4.9818	0.02995 *
time:depth	1	0.08729	0.087293	4.5553	0.03755 *
time:mesocosm	1	0.01907	0.019067	0.9950	0.32314
depth:mesocosm	1	0.00307	0.003067	0.1600	0.69077
time:depth:mesocosm	1	0.01569	0.015687	0.8186	0.36975
Residuals	52	0.99646	0.019163		

```
---
Signif. codes:  0 '***' 0.001 '**' 0.01 '*' 0.05 '.' 0.1 ' ' 1
```

- ***RI: Subsurface water ANCOVA in SAS with Tukey's HSD***

Dependent Variable: ri

Source	DF	Sum of Squares	Mean Square	F Value	Pr > F
Model	30	0.94830305	0.03161010	3.25	0.0010
Error	29	0.28207383	0.00972668		
Corrected Total	59	1.23037687			

R-Square	Coeff Var	Root MSE	ri Mean
0.770742	14.03113	0.098624	0.702894

Source	DF	Type I SS	Mean Square	F Value	Pr > F
mesocosm	1	0.09546420	0.09546420	9.81	0.0039
time	5	0.17419112	0.03483822	3.58	0.0121
time*depth	24	0.67864772	0.02827699	2.91	0.0034

Source	DF	Type III SS	Mean Square	F Value	Pr > F
mesocosm	1	0.09546420	0.09546420	9.81	0.0039
time	5	0.17419112	0.03483822	3.58	0.0121
time*depth	24	0.67864772	0.02827699	2.91	0.0034

Tukey's Studentized Range (HSD) Test for ri

Alpha	0.05
Error Degrees of Freedom	29
Error Mean Square	0.009727
Critical Value of Studentized Range	2.89239
Minimum Significant Difference	0.0521

Means with the same letter are not significantly different.

Tukey Grouping	Mean	N	mesocosm
A	0.74278	30	M2
B	0.66301	30	M1

Tukey's Studentized Range (HSD) Test for ri

Alpha	0.05
Error Degrees of Freedom	29
Error Mean Square	0.009727
Critical Value of Studentized Range	4.31120
Minimum Significant Difference	0.1345

Means with the same letter are not significantly different.

Tukey Grouping	Mean	N	time
A	0.76790	10	6
A	0.74966	10	1
B A	0.73083	10	3
B A	0.69497	10	5
B A	0.66422	10	4
B	0.60979	10	2

Level of time	Level of depth	N	ri Mean	ri Std Dev
1	0	2	0.76178785	0.05660940
1	3	2	0.78789466	0.03099579
1	5	2	0.75629968	0.07355700
1	8	2	0.56215501	0.16854943
1	1.5	2	0.88013797	0.08025695
2	0	2	0.75437472	0.03539702
2	3	2	0.63682616	0.07146349
2	5	2	0.42287085	0.15433964
2	8	2	0.69341782	0.03374758
2	1.5	2	0.54147434	0.02975319
3	0	2	0.77148699	0.18286868
3	3	2	0.47657828	0.08968245
3	5	2	0.65903647	0.14756981
3	8	2	0.84013749	0.10859972
3	1.5	2	0.90689572	0.13166935
4	0	2	0.77465280	0.20084986
4	3	2	0.55484636	0.05441609
4	5	2	0.70682634	0.19238035
4	8	2	0.70573809	0.16584712
4	1.5	2	0.57902901	0.01654836
5	0	2	0.76778002	0.12264114
5	3	2	0.62898002	0.13349123
5	5	2	0.62006684	0.13606739
5	8	2	0.76676912	0.04861842
5	1.5	2	0.69125647	0.01455350
6	0	2	0.57801329	0.04313302
6	3	2	0.84667805	0.14530972
6	5	2	0.78153803	0.07310444
6	8	2	0.82815138	0.08053829
6	1.5	2	0.80512209	0.10801778

- ***FI: Surface water ANOVA in R***

```
> x <- read.csv("FIs.csv")
> attach(x)
> y <- aov(fi~time*depth*mesocosm)
> summary(y)
```

	Df	Sum Sq	Mean Sq	F value	Pr(>F)
time	1	0.0017143	0.00171429	3.2501	0.09657 .
mesocosm	2	0.0016333	0.00081667	1.5483	0.25224
time:mesocosm	2	0.0001229	0.00006143	0.1165	0.89106
Residuals	12	0.0063295	0.00052746		

Signif. codes: 0 '***' 0.001 '**' 0.01 '*' 0.05 '.' 0.1 ' ' 1

- ***FI: Surface water ANCOVA in SAS with Tukey's HSD***

There is no significance.

- ***FI: Subsurface water ANOVA in R***

```
> x <-read.csv("FI.csv")
> attach(x)
> y <- aov(fi~time*depth*mesocosm)
> summary(y)
```

	Df	Sum Sq	Mean Sq	F value	Pr(>F)
time	1	0.000357	0.00035714	0.3868	0.5367
depth	1	0.001750	0.00175005	1.8955	0.1745
mesocosm	1	0.000327	0.00032667	0.3538	0.5545
time:depth	1	0.001687	0.00168704	1.8273	0.1823
time:mesocosm	1	0.000165	0.00016514	0.1789	0.6741
depth:mesocosm	1	0.000482	0.00048210	0.5222	0.4732
time:depth:mesocosm	1	0.000216	0.00021561	0.2335	0.6309
Residuals	52	0.048010	0.00092326		

- ***FI: Subsurface water ANCOVA in SAS with Tukey's HSD***

There is no significance.

- ***SUVA: Surface water ANOVA in R***

```
> x <-read.csv("SUVAs.csv")
> attach(x)
> y <- aov(suva~time*depth*mesocosm)
> summary(y)
```

	Df	Sum Sq	Mean Sq	F value	Pr(>F)
time	1	1.17825	1.17825	5.4950	0.03710 *
mesocosm	2	1.65634	0.82817	3.8624	0.05070 .
time:mesocosm	2	0.34938	0.17469	0.8147	0.46582
Residuals	12	2.57305	0.21442		

Signif. codes: 0 ‘***’ 0.001 ‘**’ 0.01 ‘*’ 0.05 ‘.’ 0.1 ‘ ’ 1

- ***SUVA: Surface water ANCOVA in SAS with Tukey’s HSD***

Dependent Variable: suva

Source	DF	Sum of Squares	Mean Square	F Value	Pr > F
Model	7	4.95043889	0.70720556	8.77	0.0014
Error	10	0.80658889	0.08065889		
Corrected Total	17	5.75702778			

R-Square	Coeff Var	Root MSE	suva Mean
0.859895	15.38396	0.284005	1.846111

Source	DF	Type I SS	Mean Square	F Value	Pr > F
time	5	3.29409444	0.65881889	8.17	0.0026
mesocosm	2	1.65634444	0.82817222	10.27	0.0038

Source	DF	Type III SS	Mean Square	F Value	Pr > F
time	5	3.29409444	0.65881889	8.17	0.0026
mesocosm	2	1.65634444	0.82817222	10.27	0.0038

Tukey's Studentized Range (HSD) Test for suva

Alpha	0.05
Error Degrees of Freedom	10
Error Mean Square	0.080659
Critical Value of Studentized Range	4.91202
Minimum Significant Difference	0.8054

Means with the same letter are not significantly different.

Tukey Grouping	Mean	N	time
A	2.6433	3	4
B A	2.0667	3	5
B A	1.8867	3	6
B	1.6500	3	3
B	1.4467	3	1
B	1.3833	3	2

Tukey's Studentized Range (HSD) Test for suva

Alpha	0.05
Error Degrees of Freedom	10
Error Mean Square	0.080659
Critical Value of Studentized Range	3.87678
Minimum Significant Difference	0.4495

Means with the same letter are not significantly different.

Tukey Grouping	Mean	N	mesocosm
A	2.2300	6	M2
B A	1.8200	6	MC
B	1.4883	6	M1

- ***SUVA: Subsurface water ANOVA in R***

Note: An average of the 1.5 cm SUVA values in MO replicate 2 was used for the missing data point.

```
> x <- read.csv("SUVA.csv")
> attach(x)
> y<-aov(suva~time*depth*mesocosm)
> summary(y)
```

	Df	Sum Sq	Mean Sq	F value	Pr(>F)
time	1	6.2056	6.2056	24.6777	8e-06 ***
depth	1	2.9726	2.9726	11.8212	0.001175 **
mesocosm	1	2.5661	2.5661	10.2047	0.002403 **
time:depth	1	0.4995	0.4995	1.9862	0.164807
time:mesocosm	1	0.0084	0.0084	0.0333	0.855881
depth:mesocosm	1	0.0753	0.0753	0.2996	0.586501
time:depth:mesocosm	1	0.6609	0.6609	2.6280	0.111161
Residuals	51	12.8248	0.2515		

Signif. codes: 0 ‘***’ 0.001 ‘**’ 0.01 ‘*’ 0.05 ‘.’ 0.1 ‘ ’ 1

- ***SUVA: Subsurface water ANCOVA in SAS with Tukey’s HSD***

Class	Levels	Values
time	6	1 2 3 4 5 6
depth	5	0 3 5 8 1.5
mesocosm	2	M1 M2

Number of Observations Read	59
Number of Observations Used	59

Dependent Variable: suva

Source	DF	Sum of Squares	Mean Square	F Value	Pr > F
Model	10	13.59014635	1.35901463	5.34	<.0001
Error	48	12.22311806	0.25464829		
Corrected Total	58	25.81326441			

R-Square	Coeff Var	Root MSE	suva Mean
0.526479	23.64061	0.504627	2.134576

Source	DF	Type I SS	Mean Square	F Value	Pr > F
mesocosm	1	2.75806717	2.75806717	10.83	0.0019
time	5	7.75526177	1.55105235	6.09	0.0002
depth	4	3.07681741	0.76920435	3.02	0.0266

Source	DF	Type III SS	Mean Square	F Value	Pr > F
mesocosm	1	2.50901657	2.50901657	9.85	0.0029
time	5	7.88283672	1.57656734	6.19	0.0002
depth	4	3.07681741	0.76920435	3.02	0.0266

Tukey's Studentized Range (HSD) Test for suva

Alpha	0.05
Error Degrees of Freedom	48
Error Mean Square	0.254648
Critical Value of Studentized Range	2.84347
Minimum Significant Difference	0.2642
Harmonic Mean of Cell Sizes	29.49153

Means with the same letter are not significantly different.

Tukey Grouping	Mean	N	mesocosm
A	2.3545	29	M2
B	1.9220	30	M1

Tukey's Studentized Range (HSD) Test for suva

Alpha	0.05
Error Degrees of Freedom	48
Error Mean Square	0.254648
Critical Value of Studentized Range	4.19724

Comparisons significant at the 0.05 level are indicated by ***.

time Comparison	Difference Between Means	Simultaneous 95% Confidence Limits		
6 - 4	0.1670	-0.5028	0.8368	
6 - 5	0.3560	-0.3138	1.0258	
6 - 3	0.8610	0.1912	1.5308	***
6 - 1	0.8620	0.1922	1.5318	***
6 - 2	0.9096	0.2214	1.5977	***
4 - 6	-0.1670	-0.8368	0.5028	
4 - 5	0.1890	-0.4808	0.8588	
4 - 3	0.6940	0.0242	1.3638	***
4 - 1	0.6950	0.0252	1.3648	***
4 - 2	0.7426	0.0544	1.4307	***
5 - 6	-0.3560	-1.0258	0.3138	
5 - 4	-0.1890	-0.8588	0.4808	
5 - 3	0.5050	-0.1648	1.1748	
5 - 1	0.5060	-0.1638	1.1758	
5 - 2	0.5536	-0.1346	1.2417	
3 - 6	-0.8610	-1.5308	-0.1912	***
3 - 4	-0.6940	-1.3638	-0.0242	***
3 - 5	-0.5050	-1.1748	0.1648	
3 - 1	0.0010	-0.6688	0.6708	
3 - 2	0.0486	-0.6396	0.7367	
1 - 6	-0.8620	-1.5318	-0.1922	***
1 - 4	-0.6950	-1.3648	-0.0252	***
1 - 5	-0.5060	-1.1758	0.1638	
1 - 3	-0.0010	-0.6708	0.6688	
1 - 2	0.0476	-0.6406	0.7357	
2 - 6	-0.9096	-1.5977	-0.2214	***
2 - 4	-0.7426	-1.4307	-0.0544	***
2 - 5	-0.5536	-1.2417	0.1346	
2 - 3	-0.0486	-0.7367	0.6396	
2 - 1	-0.0476	-0.7357	0.6406	

Tukey's Studentized Range (HSD) Test for suva

Alpha	0.05
Error Degrees of Freedom	48
Error Mean Square	0.254648
Critical Value of Studentized Range	4.00812

Comparisons significant at the 0.05 level are indicated by ***.

depth Comparison	Difference Between Means	Simultaneous 95% Confidence Limits		
8 - 5	0.1108	-0.4730	0.6947	
8 - 3	0.4042	-0.1797	0.9880	
8 - 1.5	0.4855	-0.1115	1.0825	
8 - 0	0.5908	0.0070	1.1747	***
5 - 8	-0.1108	-0.6947	0.4730	
5 - 3	0.2933	-0.2905	0.8772	
5 - 1.5	0.3746	-0.2224	0.9716	
5 - 0	0.4800	-0.1039	1.0639	
3 - 8	-0.4042	-0.9880	0.1797	
3 - 5	-0.2933	-0.8772	0.2905	
3 - 1.5	0.0813	-0.5157	0.6783	
3 - 0	0.1867	-0.3972	0.7705	
1.5 - 8	-0.4855	-1.0825	0.1115	
1.5 - 5	-0.3746	-0.9716	0.2224	
1.5 - 3	-0.0813	-0.6783	0.5157	
1.5 - 0	0.1054	-0.4916	0.7024	
0 - 8	-0.5908	-1.1747	-0.0070	***
0 - 5	-0.4800	-1.0639	0.1039	
0 - 3	-0.1867	-0.7705	0.3972	
0 - 1.5	-0.1054	-0.7024	0.4916	